Trends in Analytical Chemistry 189 (2025) 118246

Contents lists available at ScienceDirect

Trends in Analytical Chemistry

journal homepage: www.elsevier.com/locate/trac

Advances in DNA damage detection: Current progress, challenges, and future directions

Heeseok Kang [a,b,1], Hyung Joon Park [a,b,1], Jieun Kang [c,1], Yuna Hwang [c,d], YongJin Lee [a,b], Sang-Uk Park [e], Jeongkyu Kim [e,*], Kwan Hyi Lee [a,b,**], Sunbok Jang [c,d,***]

[a] Center for Advanced Biomolecular Recognition, Biomedical Research Division, Korea Institute of Science and Technology (KIST), Seoul, 02792, Republic of Korea
[b] KU-KIST Graduate School of Converging Science and Technology, Korea University, Seoul, 02481, Republic of Korea
[c] College of Pharmacy, Graduate School of Pharmaceutical Sciences, Ewha Womans University, Seoul, 03760, Republic of Korea
[d] Graduate Program in Innovative Biomaterials Convergence, Ewha Womans University, Seoul, 03760, Republic of Korea
[e] Department of Life Science, Chung-Ang University, Seoul, 06794, Republic of Korea

ARTICLE INFO

Keywords:
DNA damage
DNA repair
Biomarkers
Measurement techniques
Personalized medicine
Biosensors

ABSTRACT

DNA is much continuously exposed to endogenous and exogenous agents that induce damage, potentially leading to genomic instability, disease development, and aging. Detecting DNA damage and understanding associated repair mechanisms are essential for advancing diagnostic techniques, biosensors, and therapeutic interventions. Since DNA damage varies, the desired measurement approach differs, highlighting the need for an unbiased exploration of DNA damage biomarkers, along with a critical analysis of various quantification methods. Therefore, this review aims to provide a comprehensive overview of current methodologies for measuring DNA damage, focusing on direct detection of DNA lesions and indirect measurement of repair enzymes. We discuss various analytical, biochemical, and imaging techniques, identify the limitations in existing technologies and suggest future directions. This review emphasizes the growing need for advanced tools to measure DNA damage, which is set to play a transformative role in early disease detection, optimizing treatments, and supporting safe human space exploration.

1. Introduction

DNA damage is a ubiquitous event originating from endogenous metabolic processes and exogenous environmental factors, including radiation, chemicals, and ultraviolet (UV) light. If unrepaired, these damages can compromise genomic integrity, leading to mutations, cellular dysfunction, and various diseases such as cancer, neurodegenerative disorders, and aging-related conditions [1–4]. To mitigate these threats, cells have evolved complex repair mechanisms, including BER, NER, and DSB repair, each specialized to address specific types of DNA damage [5] (see Table 3)

As advancements in genomics and molecular biology research continue, the ability to accurately detect and quantify DNA damage has become essential. Beyond foundational biological research, assessing DNA damage and repair has significant implications across clinical diagnostics, environmental monitoring, and space medicine. Clinically, early detection of DNA damage can aid in diagnosing diseases such as cancer and predicting patient response to therapies, particularly those targeting DNA repair pathways [5–7]. In environmental studies, monitoring DNA damage induced by pollutants or radiation offers insight into ecosystem health and public safety [8]. For space exploration, understanding DNA damage owing to cosmic radiation is essential for ensuring astronaut safety during prolonged missions [9,10]. Given the diverse applications, it is crucial to understand the various DNA damage biomarkers suited for each specific purpose. Furthermore, since the appropriate measurement approach varies depending on the primary objective—such as precision screening or real-time monitoring—it is essential to conduct a comprehensive study that is not limited by

* Corresponding author. Department of Life Science, Chung-Ang University, Seoul, 06794, Republic of Korea
** Corresponding author. Center for Advanced Biomolecular Recognition, Biomedical Research Division, Korea Institute of Science and Technology (KIST), Seoul, 02792, Republic of Korea.
*** Corresponding author. College of Pharmacy, Graduate School of Pharmaceutical Sciences, Ewha Womans University, Seoul, 03760, Republic of Korea.
E-mail addresses: kimj@cau.ac.kr (J. Kim), kwanhyi@kist.re.kr (K.H. Lee), sunbok.jang@ewha.ac.kr (S. Jang).
[1] These authors contributed equally to this work.

https://doi.org/10.1016/j.trac.2025.118246
Received 21 November 2024; Received in revised form 7 March 2025; Accepted 26 March 2025
Available online 27 March 2025

damage type or detection method.

This review aims to provide a comprehensive overview of contemporary methodologies for detecting and measuring DNA damage and repair processes. Chapter 2 classifies DNA damage into three types based on their repair pathways: oxidative damage, UV-induced modifications, and DSBs. It details the application of techniques such as high-performance liquid chromatography (HPLC), mass spectrometry (MS), polymerase chain reaction (PCR), and advanced imaging methods for accurately measuring these damages. Conversely, Chapter 3 focuses on DNA repair biomarkers, such as enzymes and proteins, using biosensors, fluorescence, and immunoassays to assess enzymatic activities rather than direct DNA damage. The review highlights direct DNA lesion detection (Chapter 2) and indirect repair enzyme measurement (Chapter 3), providing various methods and critically evaluating their respective advantages and limitations. Moreover, Chapter 4 discusses the clinical applications of DNA damage detection, including cancer diagnostics, targeted therapy, treatment efficacy monitoring, and the study of aging and age-related diseases.

In this review, we hope to present the current landscape of DNA damage detection technologies and their applications, while also suggesting future directions for developing highly sensitive, real-time biosensors. These innovations are expected to significantly enhance disease diagnosis, treatment personalization, and the management of age-related diseases. Furthermore, as space exploration advances beyond the orbit of the Earth, robust systems for monitoring DNA integrity will be essential for the prolonged sustainability of human space exploration.

2. DNA damage-related markers and their measurement

While numerous types of DNA damage exist, the feasibility of measurement varies owing to their different aspects of structural and chemical changes. Base mismatches, commonly induced by replication stress, lead to subtle structural alterations in the DNA helix, making it challenging to differentiate them from normal base pairs, thereby complicating damage detection [11]. Conversely, DNA damage types such as bulky lesions crosslinks or single-strand breaks involve significant chemical and structural alterations induced by oxidation, alkylation, and deamination, making them easier to detect compared to those of base mismatches [5]. DSBs, where both DNA strands are simultaneously severed, require specialized measurement strategies [12]. Since directly measuring the break is challenging, alternative methods focus on identifying associated byproducts. Given the specificity of each damage type, direct measurements of biomarkers for DNA damage that can be repaired by the NER or BER pathways or result from DSBs are discussed in this chapter. Table 1 summarizes the methodologies employed to measure these types of DNA damage (see Fig. 1).

2.1. Measurement of markers repaired via the BER pathway – single-base lesions

Single-strand breaks can arise from various factors, including exposure to ionizing radiation, certain chemicals, or errors during DNA replication or repair processes. These breaks often lead to oxidation, alkylation, base deamination, or the excision of purines (adenine and guanine) and pyrimidines (cytosine and thymine). In this context, measurement approaches should focus on identifying the chemical and structural changes in DNA. Fig. 2a–e shows representative approaches for measuring damage markers repaired via the BER pathway.

One result type is the oxidation of nucleobases such as 8-hydroxy-2′-deoxyguanosine (8-OHdG), formamidopyrimidine (FapyG), and thymine glycol. In aerobic organisms, reactive oxygen species (ROS) are continuously generated in living cells owing to metabolic, physiological, and other biochemical activities. While ROS plays essential roles, their reactivity can damage DNA by generating additional radicals within DNA bases, leading to oxidation products [13,14]. Among these, 8-OHdG—which forms from guanine oxidation—is the most extensively

Table 1
Summary of DNA damage biomarkers, their corresponding detection methods, and findings regarding sensitivity and detection limit.

Damage type	Biomarker	Method	Findings	Ref.
Single-base lesions	8-OHdG	HPLC-ECD	Detected urinary 8-OHdG with nanogram-level detection limit per mL.	[19]
Single-base lesions	8-OHdG	HPLC- ECD	Measured salivary 8-OHdG in non-smokers averaged 3.80 ng/mL with a detection limit of <0.2 ng/mL, and the levels were significantly higher in smokers.	[17]
Single-base lesions	8oxoG	HPLC	Sufficient resolution for 8-oxoG can be achieved with at least 100 μg of DNA.	[50]
Single-base lesions	8-OHdG	HPLC- ECD combined with SPE	Quantified human serum 8-OHdG with low LOD <10 pg/mL.	[18]
Single-base lesions	8-OHdG	LC-MS	Identified one oxidized deoxyguanosine per 5×10^5 deoxyguanosine.	[51]
Single-base lesions	FapyG	HPLC, GCMS, COMET	Identified FapyGua lesions in DNA with a detection limit of 3 FapyGua per 10^6 bases.	[22]
Single-base lesions	Thymine glycol	32P	32P-postlabeling assay to identify radiogenic DNA damage, identifying that thymine glycols are formed in irradiated DNA with a G value of 0.0022 μmol J^{-1}.	[52]
Single-base lesions	Thymine glycol	GC-MS	Identified thymidine glycol in DNA, achieving a detection limit of 41 amol and measuring background levels of 11.7×10^{-6} mol thymidine glycol per mol thymidine in undamaged DNA.	[26]
Single-base lesions	Thymine glycol	LC-MS	Achieved LOD of one lesion per three million nucleotides, with sensitivity high enough to measure as little as 1 pmol.	[53]
Single-base lesions	Thymine glycol	Capillary electrophoresis and laser-induced fluorescence	Detected thymine glycol with a detection limit of 3 $\times 10^{-21}$ mol and observed enhanced repair in A549 cells post low-dose radiation exposure.	[27]
Single-base lesions	Uracil	Real-time PCR	Quantified uracil with a sensitivity of 1000 uracils per million bases, improved with longer DNA fragments.	[29]

(continued on next page)

Table 1 (*continued*)

Damage type	Biomarker	Method	Findings	Ref.
Single-base lesions	Hypoxanthine	Aggregation luminogen	Achieved LOD of 1.2 μM with a linear range of 5–120 μM.	[30]
Single-base lesions	Hypoxanthine	Carbon paste electrode	Achieved linear response in the range of 1–0.4 mM with a LOD of 0.8 mM.	[32]
Single-base lesions	Hypoxanthine	Colorimetric assay	Achieved linear range of 2.50–153.1 mg/kg with a LOD of 1.84 mg/kg, applied to the detection of Hx in an aquatic product.	[33]
Single-base lesions	Hypoxanthine	HPLC	Achieved LOD of 0.5 μmol/L and capable of simultaneous determination of hypoxanthine and xanthine in biofluid.	[54]
Single-base lesions	Hypoxanthine	Smartphone	Multicolor sensing method with LOD of 0.378 μM, enabling rapid on-site freshness assessment of aquatic products.	[31]
Single-base lesions	AP sites	Formation, detection	Achieved LOD of 1 AP site per 10^6 bases using [14C] methoxyamine labeling.	[55]
Single-base lesions	AP sites	ARP assay	Achieved sensitivity of one AP site per 10^4–10^5 bases, which can be enhanced to one AP site per 10^6 bases using a nitrocellulose membrane.	[37]
Single-base lesions	AP sites	ARP assay	ARP-slot blot assay reached an LOD of 0.24 AP sites per 10^6 nucleotides.	[56]
Single-base lesions	AP sites	ARP assay	Achieved LOD of one AP site per 10^4 nucleotides, equivalent to 15 fmol.	[57]
Bulky lesions	6-4 PP	LM- PCR	Detected as few as 100 DNA molecules.	[40]
Bulky lesions	6-4 PP, CPD	Fluorescent-labeling	Used fluorescently labeled photolyases to detect CPDs and 6-4 PPs in live cells at a detection threshold as low as 1 J/m^2.	[42]
Bulky lesions	6-4 PP, CPD	LM- PCR	Had a sensitivity of detecting as low as 0.5 CPD or 6-4 PP lesions per 10^6 nucleotides.	[58]
Bulky lesions	6-4 PP, CPD	LC-MS, Immunoassay	LOD as low as 0.1 J/m^2 of UV exposure.	[38]
Bulky lesions	CPD	Comet Assays	Measured the damage at the single-cell level.	[59]
Bulky lesions	CPD	LM- PCR	Detection sensitivity of 600 J/m^2 of UV exposure.	[60]
Bulky lesions	CPD	Near-infrared radiation	Aquaphotomics was able to detect with LOD of 0.77 μM for *cis*-syn thymine dimers.	[61]
Bulky lesions	CPD	Oligonucleotides with magnetic beads	Detected at the nucleotide level, improving specificity and reducing background labeling in DNA samples.	[62]
Bulky lesions	CPD	Sensitive nonradioactive	Detected in mammalian cells, LOD as low as 0.1 J/m^2 of UV exposure.	[63]
DSB	γ-H2AX	Fluorescence detection	Detected with a sensitivity down to 0.5 Gy of radiation exposure.	[47]
DSB	γ-H2AX	IR dose response	Detected with a sensitivity of 0.02 Gy of ionizing radiation in human lymphocytes.	[46]
DSB	γ-H2AX	Laser scanning cytometry	Detected γH2AX foci in buccal cells with a detection sensitivity down to 1 Gy of ionizing radiation exposure.	[48]
DSB	γ-H2AX	Flow cytometry, western blotting	Detected with a sensitivity of detecting DNA damage down to 1 Gy of radiation.	[45]

*HPLC: high-performance liquid chromatography.
* ECD: electrochemical detection.
* GC-MS: gas chromatography–mass spectrometry.
* LC-MS: liquid chromatography–mass spectrometry.
* ARP assay: aldehyde reactive probe assay.
* LM-PCR: ligation-mediated polymerase chain reaction.
* IR dose: ionizing radiation dose.
* LOD: limit of detection.
* 8-OHdG: 8-hydroxy-2′-deoxyguanosine.

studied biomarker of oxidative DNA damage, with significant implications for assessing endogenous oxidative damage to DNA and its role in initiating and promoting carcinogenesis [15,16]. HPLC is commonly used for quantitative analysis of 8-OHdG from urine or saliva and is often coupled with MS or electrochemical detection (ECD) methods to enhance accuracy and reliability (Fig. 2a) [17–19]. While commercially available enzyme-linked immunosorbent assay (ELISA) kits enable convenient detection of 8-oxoG lesions, HPLC assays with UV and ED offer more definitive identification and quantification of 8-oxoG [17]. Additionally, liquid chromatography-tandem mass spectrometry (LC-MS/MS) provides more accuracy compared to that of ELISA. However, HPLC-ECD offers a more economical and accessible option for large-scale epidemiological studies [17,20]. FapyG—another modified nucleobase that undergoes oxidative damage—exhibits even higher mutagenicity in mammalian cells compared to that of 8-OHdG [21]. HPLC, coupled with various techniques such as GC-MS, EC, and UV is used for detecting FapyG [22]. Additionally, the comet assay or single-cell gel electrophoresis, is used for measuring DNA damage. It can be calibrated using data from HPLC/GC-MS to establish background levels, yields of strand breaks, and DNA base damage from low-dose irradiation [22].

While guanine biomarkers are commonly studied regarding oxidative DNA damage, thymine also has its oxidative damage markers, with thymine glycol as a key example. This marker is significant because, if unrepaired before encountering the replication fork, it can block DNA polymerase, potentially leading to cell death [23]. Although thymine glycol exhibits low mutagenic potentials, with a low rate of T→C mutations, it strongly inhibits repair and replicative DNA polymerases *in*

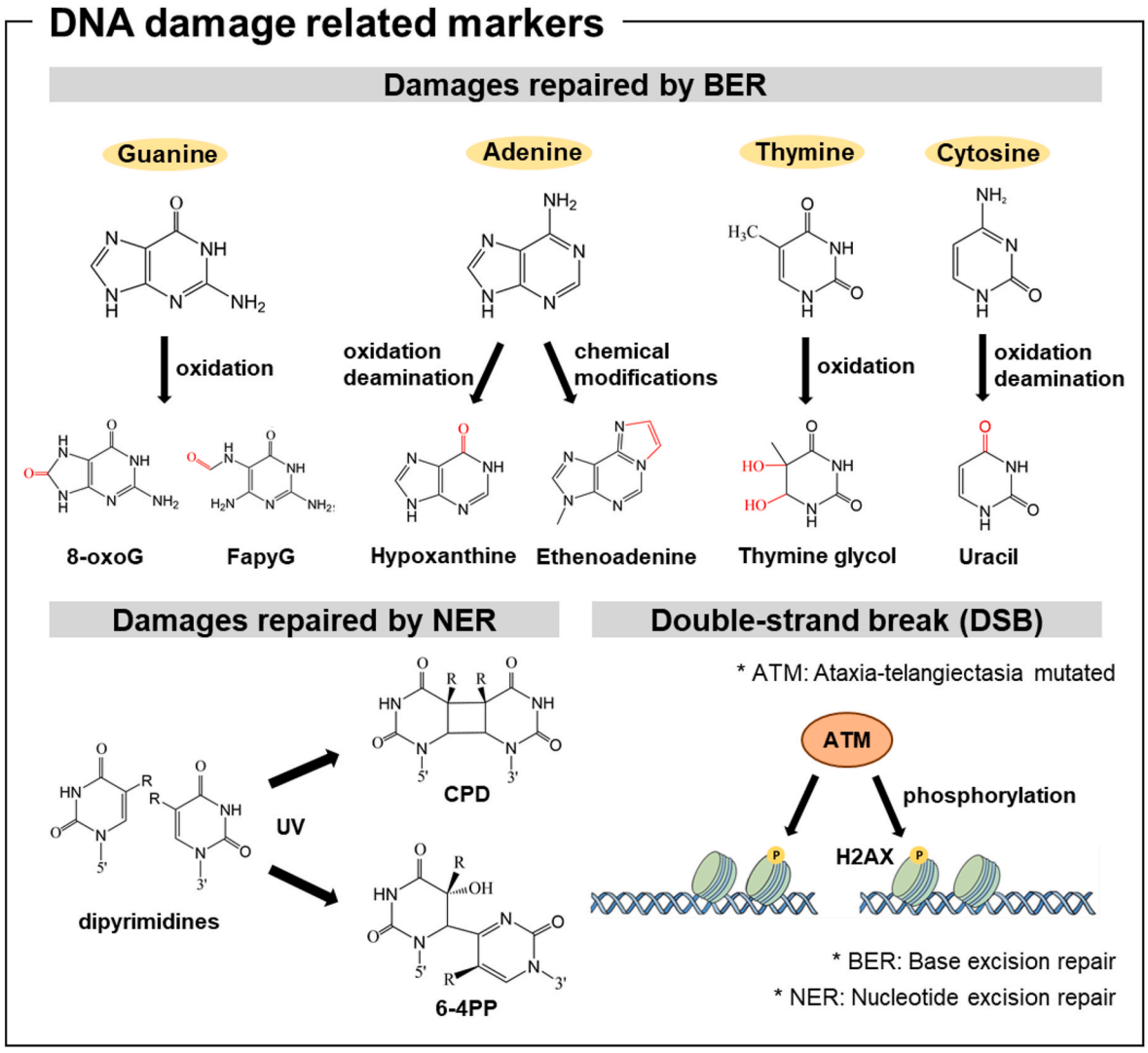

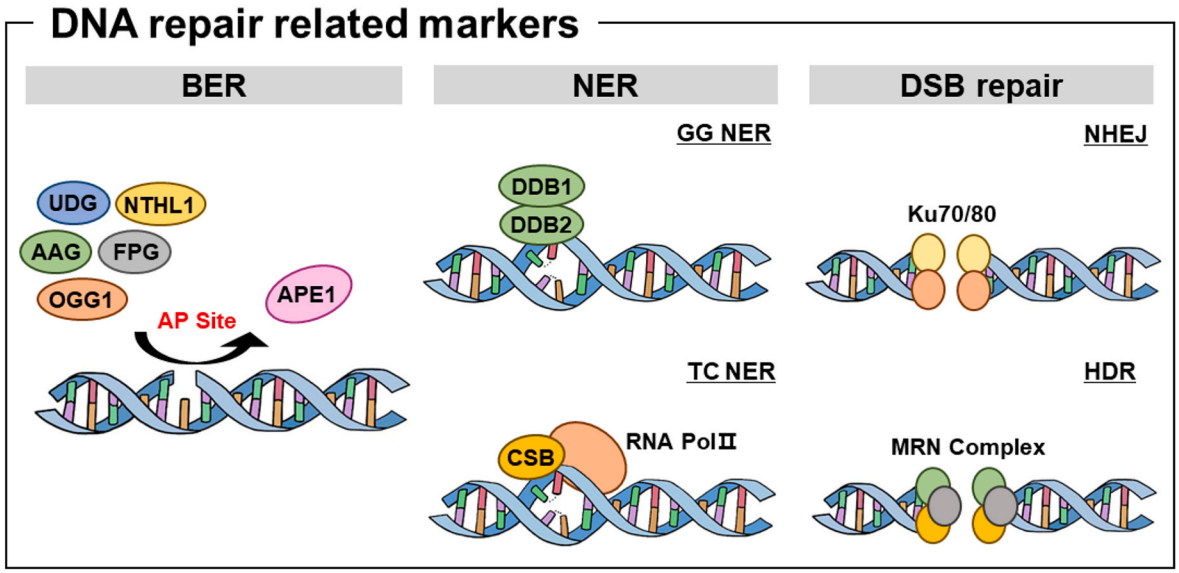

Fig. 1. Overview of DNA damage and repair-related markers. The upper section shows damages repaired by BER, resulting from oxidation, deamination, and chemical modifications; NER, which addresses UV-induced lesions; and DSBs, with the phosphorylation of H2AX by ATM kinase in response to DNA damage. The lower section highlights the involvement of various DNA repair proteins in BER, NER, and DSB repair. BER, base excision repair; NER, nucleotide excision repair; DSBs, double-strand breaks.

Single-base lesions

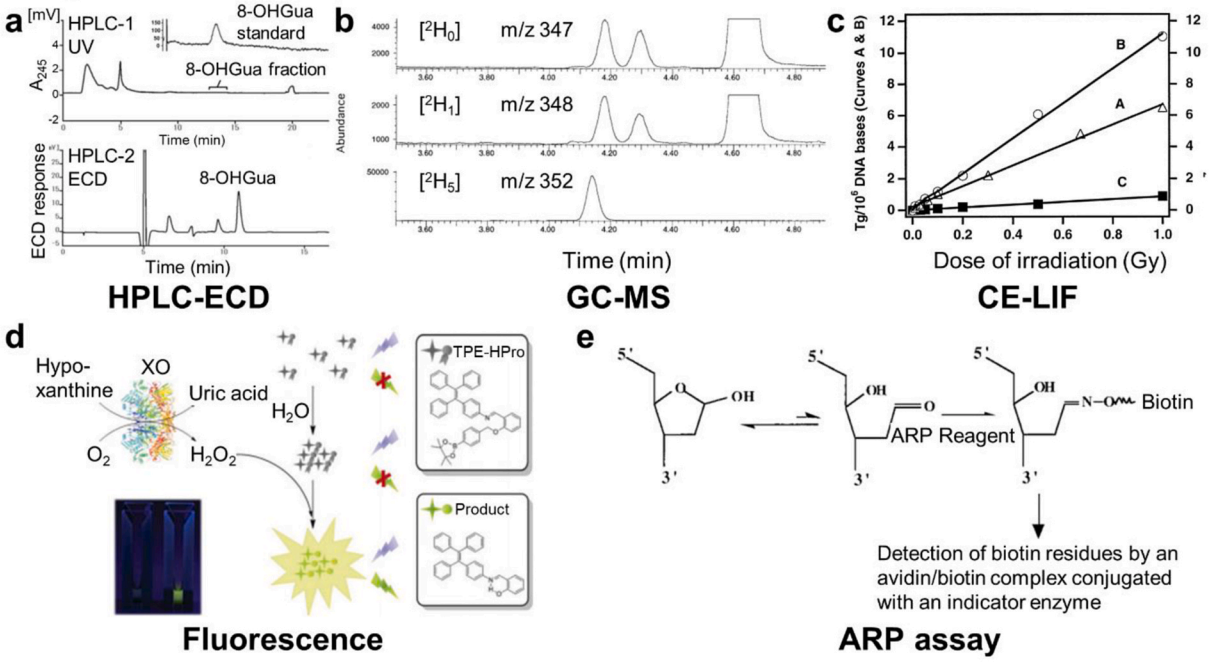

* HPLC-ECD: High-performance liquid chromatography with electrochemical detection

* ARP assay: Aldehyde reactive probe assay

* CE-LIF: Capillary electrophoresis with laser-induced fluorescence

Bulky adducts or crosslinks

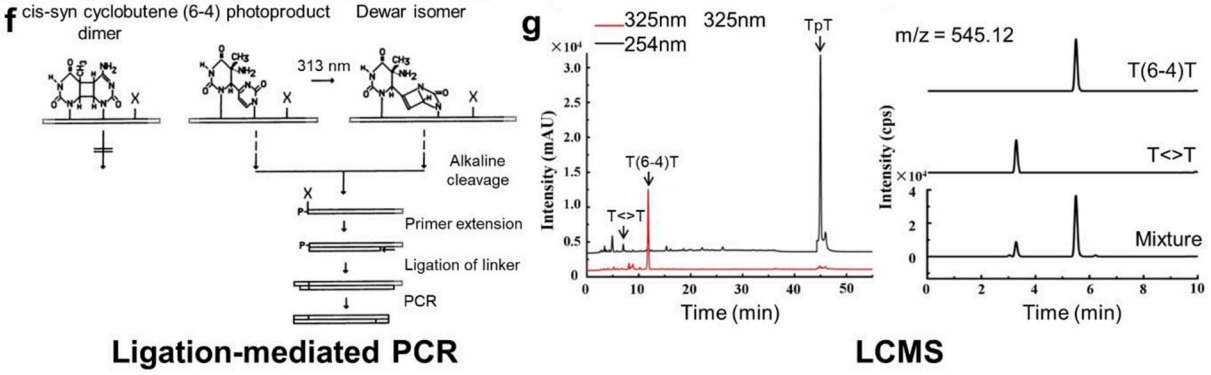

* LCMS: :Liquid Chromatography-Mass Spectrometry

Double-strand break

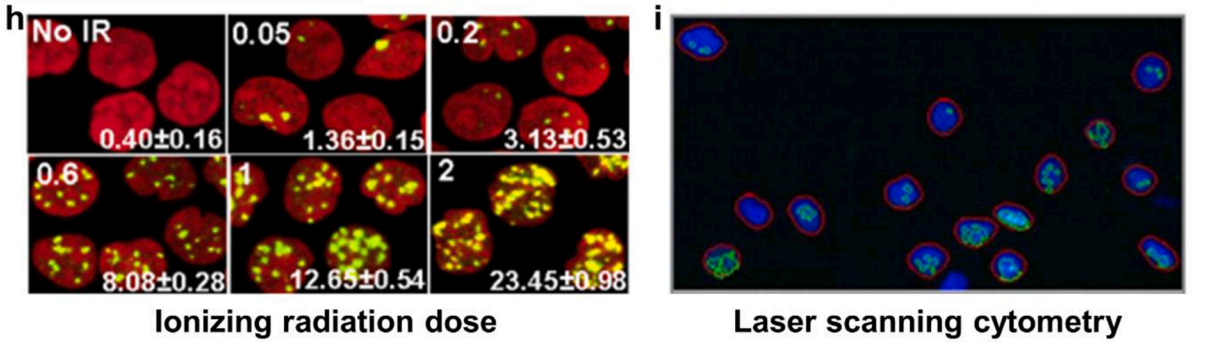

(caption on next page)

Fig. 2. Measurement of DNA damage-related markers. (a–e) Detection of damage markers repaired via BER. (a) Detected 8-OHdG in saliva via HPLC-ECD. Reproduced with permission from ref. [17]. (b) Thymine glycol measured via GC-MS, showing signals for three isotopomers: *m/z* 347 (background), *m/z* 348 (thymidine glycol), and *m/z* 352 (internal standard). Reproduced with permission from ref. [26]. (c) Thymine glycol yield from irradiated calf thymus DNA. Reproduced with permission from ref. [27]. (d) Detection of hypoxanthine using a fluorescence assay based on aggregation-induced emission luminogen. Reproduced with permission from ref. [30]. (e) Detected AP sites using biotinylated aldehyde-specific reagent, ARP, and a colorimetric ELISA-like assay to quantify biotin-tagged AP sites. Reproduced with permission from ref. [37]. (f, g) Detected UV-induced damage repaired via NER. (f) CPD and T(6-4)T photoproducts analyzed through HPLC-DAD chromatograms (left) and UHPLC-Q-TOF MS (right). Reproduced with permission from ref. [40]. (g) Outline of (6-4) photoproduct detection by LM-PCR. Reproduced with permission from ref. [38]. (h, i) Detected DSB markers. (h) γ-H2AX quantified following varying doses of ionizing radiation (IR). Reproduced with permission from ref. [46]. (i) Laser scanning cytometry used for visualization. Reproduced with permission from ref. [48]. HPLC-ECD, high-performance liquid chromatography with electrochemical detection; GC-MS, gas chromatography-mass spectrometry; AP, Abasic; ARP, aldehyde reactive probe; UV, ultraviolet; CPD, Cyclobutane pyrimidine dimers; HPLC-DAD; HPLC with diode-array detection; UHPLC-Q-TOF MS, ultra-high-performance liquid chromatography-quadrupole time-of-flight mass spectrometry; LM-PCR, ligation-mediated polymerase chain reaction; 8-OHdG, 8-hydroxy-2′-deoxyguanosine; ELISA, enzyme-linked immunosorbent assay.

vitro [24]. *In vivo,* unrepaired thymine glycol can be lethal unless bypassed by *trans*-lesion synthesis or recombination mechanism [25]. The lesion, such as guanine biomarkers, can be measured using chromatographic techniques, including LC-MS/MS or gas chromatography (GC)-MS. GC-MS is particularly valuable for identifying volatile or semi-volatile derivatives of thymine glycol following chemical derivatization. Naritsin et al. quantified thymidine glycol residues using GC/electron capture negative ionization MS, allowing for precise quantification at trace levels, making it ideal for analyzing thymine glycol in complex biological samples [26]. (Fig. 2b) To further enhance sensitivity beyond chromatographic methods, researchers combined immunochemical recognition with capillary electrophoresis and laser-induced fluorescence detection, achieving an impressive detection limit of 3×10^{-21} mol. Le et al. demonstrated that lower radiation doses (starting at 0.01 Gy) generate detectable levels of thymine glycol [27]. (Fig. 2c) Such advanced techniques surpass traditional chromatographic limits, offering valuable tools for studying DNA damage under low-dose radiation or other subtle oxidative stress conditions.

The second type of damage involves the deamination of nucleobases, with uracil and hypoxanthine as representative markers. Uracil arises from the deamination of cytosine, while hypoxanthine forms from that of adenine. The accumulation of these markers can also contribute to carcinogenesis and genomic instability [28]. Horvath et al. introduced a quantitative method for assessing uracil in DNA using a real-time PCR assay [29]. This method uses wild-type *Pyrococcus furiosus* DNA polymerase, which binds strongly to uracil and stalls on uracil-containing templates, enabling direct measurement of uracil content. However, as discussed in Chapter 3, indirect approaches, such as detecting uracil-DNA glycosylase (UDG), are more commonly studied for uracil measurement.

Hypoxanthine possesses unique characteristics, serving as a marker of intracellular energy status or certain pathological conditions and as a marker of freshness in aquatic products, especially during the early stages of spoilage [30,31]. Consequently, various sensing techniques have been developed for its detection, including fluorescence, electrochemical methods, chemiluminescence, and electrochemiluminescence [30]. Hu et al. developed a carbon paste electrode for detecting hypoxanthine using cyclic voltammetry [32]. This sensor utilizes a sodium montmorillonite-methyl viologen-modified carbon paste electrode, where oxygen consumption during the enzymatic reaction is used to quantify hypoxanthine within a linear response range of 1–0.4 mM. Fig. 2d shows a fluorometric assay using an aggregation-induced emission active fluorescent luminogen, which detects and quantifies hypoxanthine in a “turn-on” manner [30]. This method demonstrates high sensitivity with a linear range extending up to 120 mM and a limit of detection (LOD) of 1.2 mM, which aligns well with endogenous hypoxanthine levels in human plasma and urine. Additionally, colorimetric approaches have been developed, utilizing the peroxidase-like activity of Co-doped g-C_3N_4 or the specific properties of manganese dioxide (MnO_2) nanosheets, which oxidize colorless 3,3′,5,5′-tetramethylbenzidine (TMB) into yellow TMB^{2+} [31,33]. These colorimetric methods can now be applied in smartphone-based applications, enabling convenient and portable hypoxanthine detection [31].

Unlike the previous two types of DNA damage, which arise from oxidation or deamination involving chemical modification, AP sites represent a DNA damage type characterized by structural changes owing to the loss of a DNA base [34]. The aldehyde reactive probe (ARP) assay (Fig. 2e) is a predominantly used method for measuring AP sites. ARP specifically reacts with the open-ring aldehyde group of the deoxyribose sugar at AP sites, forming a stable ARP-DNA adduct [35,36]. The ARP-labeled DNA can be identified by binding it to streptavidin conjugated with horseradish peroxidase (HRP) and incubating it with a chemiluminescent substrate for an optical readout. Alternatively, the DNA can be directly bound to fluorescently tagged streptavidin for fluorescence measurement, or click chemistry can be employed to replace biotin with a fluorescent dye, such as Cy5 [36,37]. These colorimetric, fluorometric, or chemiluminescent readouts provide simple, rapid, and sensitive means to measure AP sites.

2.2. Measurement of markers repaired via the NER pathway – bulky lesions

When DNA is exposed to external stimuli such as UV light, damage can result in covalent bond formation on pyrimidine bases, such as thymine and cytosine. This bonding leads to the creation of cyclobutane pyrimidine dimers (CPDs). If bonding occurs between the carbon at position 6 of one pyrimidine base and at position 4 of an adjacent pyrimidine base, respectively, it forms 6-4 photoproducts (6-4 PPs) [38]. These lesions are highly mutagenic and play a significant role in developing skin cancer, making their detection essential [39]. PCR, LC-MS, immunoassay, and fluorescent labeling serve as representative approaches for measurement. Fig. 2f and g shows some examples.

Fig. 2f shows the ligation-mediated PCR (LM-PCR) method developed by Pfeifer et al. for detecting 6-4 PPs, demonstrating its potential to map adduct frequency at single-nucleotide resolution in single-copy genes of mammalian cells [40]. Moreover, Lai et al. suggest the use of UHPLC-MS/MS, which allows differentiation and characterization of these pyrimidine dimer lesions despite their identical molecular weights [38]. (Fig. 2g) Additionally, for high-sensitive assays, the immune-slot blot technique can be employed to identify or quantify DNA adducts using specific monoclonal antibodies (if available), ensuring no cross-reactivity with normal or altered DNA nucleobases [41]. However, despite their high sensitivity, these methods are limited to endpoint measurements and are not suitable for real-time monitoring of DNA damage within living cells [42].

To address this limitation, Barbara et al. developed a novel method using fluorescently-tagged photolyases to directly recognize and quantify UV-induced DNA damage with high sensitivity in living cells. This method not only allows for efficient identification of UV-induced DNA damage without inhibiting NER activity but also enables immediate reversal of DNA damage using 405 nm laser-assisted photo-reactivation during live-cell imaging. These advancements offer novel possibilities for real-time DNA damage repair in cellular contexts.

2.3. Measurement of byproducts from DSBs

DNA DSBs can arise within biological systems owing to various factors, including replication stress, endogenous ROS, and exposure to exogenous sources such as ionizing radiation and genotoxic compounds [12]. In response to these lesions, the DNA damage response mechanism is rapidly activated at the specific damage site. One of the earliest cellular responses to DSBs is phosphorylation of the histone protein H2AX at its C-terminal region, referred to as γ-H2AX, upon phosphorylation [43]. Two primary approaches are commonly used to measure γ-H2AX, namely microscopy-based and cytometry-based techniques.

Fluorescence microscopy allows for visualizing γ-H2AX foci by immunostaining cells with primary γ-H2AX antibodies, followed by fluorescently labeled secondary antibodies. A significant advantage of this method is its ability to identify solitary DNA DSBs within single cells [44]. Furthermore, fluorescence-based, such as western blotting and flow cytometry, can be used to quantify overall γ-H2AX protein levels across various cell types and tissues [45]. In radiation biology, a well-established positive correlation exists between the number of DNA DSBs and γ-H2AX foci formation. A study demonstrates a linear increase in γ-H2AX foci per cell, which directly correlated with the initial radiation doses of 0.2–5 Gy, observed at 24-h and 48-h post-exposure in human blood samples and skin cells [46]. (Fig. 2h)

Flow cytometry enables rapid quantification of overall γ-H2AX intensity across different cell populations, facilitating the assessment of γ-H2AX levels across various cell cycle phases [47]. This technique also enables the simultaneous measurement of additional cellular proteins or markers involved in DNA damage and repair pathways. In lymphocytes, flow cytometry-based quantification of γ-H2AX intensity shows a qualitative correlation with the number and size of γ-H2AX foci, which are

Table 2
Summary of DNA repair enzymes, detection methods, and findings regarding sensitivity and limit of detection.

Damage type	Lesion	Enzyme	Method	Findings	Ref.
Single-base lesions	8-OHdG	OGG1	Fluorescence-based assay	Fluorescence emission triggered by OGG1 activity on 8-OHdG-labeled DNA duplex.	[66]
Single-base lesions	8-OHdG	OGG1	CRISPR-Cas12a based biosensor	Removal of 8-OHdG initiates SDA and Cas12a activation, producing fluorescence with a detection limit of 4.24×10^{-9} U/μL in 40 min.	[67]
Single-base lesions	8-OHdG	OGG1	DNAzyme-based colorimetric assay	Lambda exonuclease releases a G-quadruplex sequence, forming a DNAzyme that generates color change with a LOD of 0.01 U/mL.	[68]
Single-base lesions	8-OHdG	OGG1	Nanopore-based sensor	OGG1 cleaves 8-OHdG, producing DNA fragments detected by current blockades with a detection limit of 6.5×10^{-3} U/mL.	[69]
Single-base lesions	FapyG	FPG	Self-primed RCA	FPG cleaves 8-OHdG, initiating RCA to amplify fluorescence with a detection limit of 1.033 U/mL.	[71]
Single-base lesions	FapyG	FPG	Fluorescent copper nanoclusters	FPG recognizes and excises 8-OHdG, producing ssDNA as a CuNC template with a detection limit of 0.01 U/mL.	[72]
Single-base lesions	FapyG	FPG	DNAzyme-assisted signal amplification	FPG activity restores fluorescence by cleaving a DNAzyme substrate with a detection limit of 0.66 U/mL.	[73]
Single-base lesions	Thymine glycol	NTHL1	FRET-based DNA probes	NTHL1 cleaves thymine glycol, disrupting FRET and increasing fluorescence to detect enzyme activity.	[74]
Single-base lesions	Uracil	UDG	Luminescent switch-on assay	UDG removes uracil, forming a G-quadruplex that activates a DID-VP probe with a LOD of 0.005 U/mL.	[77]
Single-base lesions	Uracil	UDG	qPCR-based assay	UDG removes uracil, reducing PCR amplicon yield for precise enzyme activity quantification.	[78]
Single-base lesions	Hypoxanthine	AAG	Fluorescence-based assay	AAG excises damaged bases, initiating hyperbranched DNA formation and fluorescence, with a detection limit of 0.090 U/mL.	[81]
Single-base lesions	Hypoxanthine	AAG	Quantum dot FRET nanosensor	AAG excises deoxyinosine, triggering strand displacement and a FRET signal increase, with a detection limit of 3.60×10^{-10} U/μL.	[82]
Single-base lesions	Hypoxanthine	AAG	Triple-signal amplification	AAG excises deoxyinosine, initiating triple-signal amplification with a detection limit of 0.026 U/mL.	[83]
Single-base lesions	AP sites	APE1	Fluorescent biosensor	AP site cleavage triggers TdT elongation and Endo IV cleavage, generating fluorescence with a detection limit of 1.7×10^{-6} U/mL.	[85]
Single-base lesions	AP sites	APE1	Fluorescence-based assay	APE1 cleaves the AP site, releasing ATMND and restoring fluorescence, with a detection limit of 0.04 U/mL.	[86]
Bulky adducts	CPDs and 6-4 PPs	UV-DDB	EMSA	UV-DDB binds to damaged DNA, altering gel migration to allow quantification of its binding affinity and activity.	[80]
Bulky adducts	CPDs and 6-4 PPs	UV-DDB	Chromatin digestion assay	Approximately 70 % of DDB2 localized to solubilized internucleosomal sites after UV exposure, enabling precise quantification of UV-DDB in chromatin structures.	[91]
Bulky adducts	CPDs and 6-4 PPs	CSB	Western blot	CSB protein levels were quantified using specific antibodies normalized against HSP90, providing precise CSB measurement.	[93]
Bulky adducts	CPDs and 6-4 PPs	CSB	qXR-Seq	CSB plays a critical role in excision repair, with double knockout cells showing 0.3 % repair activity compared to wild-type, underscoring its importance in DNA repair.	[95]
DSBs	DSBs	Ku heterodimer	Biochemical assays and FRAP	Ku dissociation from DNA ends was detected using pull-down assays and real-time FRAP, demonstrating the phosphorylation-dependent release of Ku from DNA.	[100]
DSBs	DSBs	Ku heterodimer	Western blot analysis and kinase assays	Ku70/Ku80 protein levels and phosphorylation status were quantified using Western blot and phosphorimager to assess dissociation and phosphorylation dynamics.	[101]
DSBs	DSBs	MRN complex	IHC	MRN complex protein levels were measured in ovarian carcinoma samples using IHC, with quantification based on nuclear staining intensity.	[102]
DSBs	DSBs	MRN complex	LC-MS/MS	MRN complex components MRE11, RAD50, and NBS1 were quantified at the molecular level using LC-MS/MS.	[104]

*RCA, rolling circle amplification.
*FRET, fluorescence resonance energy transfer.
*EMSA, electrophoretic mobility shift assay.
*qXR-Seq, quantitative excision repair sequencing.
*FRAP, fluorescence recovery after photobleaching.
*IHC, immunohistochemistry.
*LC-MS/MS, liquid chromatography-tandem mass spectrometry; CSB, Cockayne syndrome group B; UDG, uracil-DNA glycosylase; APE1, apurinic/apyrimidinic endonuclease 1; ATMND, 2-amino-5,6,7-trimethyl-1,8-naphthyridine; AAG, alkyladenine DNA glycosylase; FPG, formamidopyrimidine glycosylase.

visually assessed using fluorescence microscopy.

Laser scanning cytometry (LSC) has recently emerged as an effective method for assessing cellular DNA content to determine cell cycle stages, especially when combined with multiple γ-H2AX parameters (e.g., area, integral, and MaxPixel) following DNA damage induction [48]. In human buccal cell nuclei, visually scored γ-H2AX foci frequency strongly correlates with γ-H2AX integral measurements obtained via LSC (Fig. 2i).

In conclusion, microscopy-based and cytometry-based techniques are well-suited for assessing γ-H2AX foci formation and resolution. The selection of the most appropriate γ-H2AX assay should align with specific study goals. While image cytometry and LSC offer the advantage of quantifying and measuring the size of γ-H2AX foci, these methods tend to be slower in execution [49]. Implementing these techniques for quantifying γ-H2AX foci may also serve as early indicators of the risk for age-related diseases.

3. DNA repair-related markers and their measurement

While the previous chapter discussed direct methods for measuring DNA damage, this chapter focuses on detecting the repair enzymes that are activated in response to DNA damage, especially those involved in the initial recognition of the damage. Quantifying the activity of these recognition enzymes provides an indirect approach to quantifying the extent of DNA damage. Since the primary goal is to understand DNA damage, targeting the enzymes that serve as the first responders to this damage can offer valuable insights. This chapter outlines key enzymes in the BER, NER, and DSB pathways, emphasizing the methods used for their quantification. Table 2 provides an overview of the enzymes associated with each type of DNA damage and the corresponding methodologies employed for their quantification.

3.1. Measurement of markers involved in BER pathway

This section focuses on enzymes that recognize single-base lesions, as described in section 2.1. These enzymes initiate the BER process by identifying and removing the damaged bases, ensuring the genomic integrity is preserved [64]. Fig. 3a–d shows the methods used to measure these enzymes.

8-oxoguanine DNA glycosylase (OGG1) is a critical enzyme in the BER pathway, which is in charge of recognizing and removing 8-OHdG, further initiating the repair process by creating AP sites [65]. Various strategies have been developed to quantify and assess OGG1 activity. Visnes et al. designed a fluorescence-based assay to measure the activity of OGG1, where a synthetic DNA duplex with 8-OHdG residue, which was modified with a fluorophore and a quencher, was utilized as a reporter. As OGG1 recognizes and removes the 8-OHdG site on the reporter strand, the quencher detaches from the strand, triggering fluorescence emission of the fluorophore. Higher OGG1 activity leads to an increase in fluorescence signal. This method possesses its strength in high sensitivity, high-throughput capability, and quantitative nature, whereas the specificity and requirement of APE1—the enzyme that further processes the AP site and detaches the quencher from the strand by cleaving the strand—are the limitations [66]. Zhang et al. developed a biosensor leveraging the CRISPR-Cas system [67]. The presence of OGG1 facilitates the excision of a hairpin DNA probe containing 8-OHdG lesions, initiating a quadratic strand displacement amplification (SDA) reaction. This reaction produces activators that bind to crRNA, activating the Cas12a enzyme. The enzyme cleaves the signal probe and ultimately releases a fluorescent dye (Cy5), which makes the fluorescence signal. The method demonstrates high sensitivity with a detection limit of 4.24×10^{-9} U/μL and high specificity, and still rapid where the entire assay can be completed within 40 min. However, the use of CRISPR Cas enzyme may increase the cost and limit scalability. Liu et al. developed a colorimetric assay that employs a DNAzyme that mimics HRP activity to generate a visible signal [68]. This assay also uses DNA oligonucleotides containing 8-OHdG lesions but paired with a G-quadruplex sequence on Table 3 the complementary strand. Upon OGG1-mediated cleavage of the DNA duplex, a recessed 5′-phosphate terminus is exposed, allowing lambda exonuclease to further digest the duplex and release the G-quadruplex sequence. The released sequence then forms a complex with hemin, creating the DNAzyme, which catalyzes the oxidation of a substrate, 2,2′-azinobis(3-ethylbenzothiozoline)-6-sulfonic acid, $ABTS^{2-}$, generating a measurable colorimetric change via UV–vis spectroscopy. This method offers a low detection limit of 0.01 U/mL and does not require sophisticated techniques or equipment to conduct. Conversely, the stability of the assay performance is questionable in complex samples owing to its colorimetric nature, and the reported dynamic range by the authors is relatively narrow (0.05–32 U/mL). Fig. 3a presents a label-free method of detecting hOGG1 activity using a nanopore-based sensor introduced by Shang et al. In this method, hOGG1 cleaves the 8-OHdG lesion to create a DNA fragment that will pass through the sensor based on α-hemolysin nanopore [69]. This creates detectable current blockades, serving as the signatures of hOGG1 activity. The method demonstrates high sensitivity, with a detection limit as low as 6.5×10^{-3} U/mL, and requires no labeling or signal amplification. However, the preparation of nanopore sensors might be burdensome, limiting the throughput.

Regarding FapyG, DNA-formamidopyrimidine glycosylase (FPG) plays an essential role in recognizing and removing the damaged lesion [70]. For detecting and measuring FPG, most studies utilize 8-OHdG lesions since FPG also targets 8-OHdG as FapyG and 8-OHdG are oxidized purines. Song et al. developed a highly sensitive approach to detect FPG activity by combining self-primed rolling circle amplification (RCA) with magnetic nanoprobes [71]. The method begins with FPG binding to and cleaving an 8-OHdG lesion in a custom DNA duplex, creating 5′-phosphoryl termini. This DNA product is then ligated to form a circular strand, serving as a template for RCA. The RCA process amplifies the signal by generating long DNA strands with multiple recognition sites for fluorescently labeled probes. These amplified products are subsequently captured by magnetic nanoprobes via streptavidin-biotin interactions, leading to significant fluorescence signal accumulation. Confocal laser scanning microscopy is then used to measure the amplified fluorescence signal, achieving a sensitive detection of FPG activity with a detection limit as low as 1.033 U/mL. While this method benefits from high sensitivity and specificity through signal amplification, its multi-step protocol and potential for nonspecific binding may pose a challenge. Li et al. introduced a method that combines multi-enzyme catalysis and fluorescent copper nanoclusters (CuNCs), yielding a low detection limit of 0.01 U/mL [72]. The authors designed a DNA duplex in which, following FPG cleavage, nicks with phosphate groups are created at the 3′ and 5′ ends. These modifications allow selective action by two enzymes: lambda exonuclease (λ Exo), which digests DNA from the 5′ phosphate end, and exonuclease I (Exo I), which is inhibited by the 3′ phosphate end. Such selective digestion produces single-stranded DNA templates that serve to synthesize CuNCs, whose fluorescence serves as the detection signal for FPG activity. This method minimizes background signal noise, allowing it to detect FPG activity in complex biological samples. However, it requires multiple enzymes and involves the synthesis of fluorescent CuNCs, which can be technically demanding and time-intensive. Qiu et al. employed DNAzyme-assisted signal amplification combined with reduced graphene oxide (rGO) quenching (Fig. 3b) [73]. The method also uses a DNA substrate with an 8-OHdG lesion, which, upon cleavage by FPG, activates a DNAzyme that catalyzes the cleavage of a fluorescently labeled probe. The rGO quenches the fluorescence of the intact probe, but cleaved restores fluorescence, generating a detectable signal. This approach achieves high sensitivity, with a detection limit of 0.66 U/mL, and is adaptable to various applications. However, precise conditions for the DNAzyme and rGO are essential, potentially complicating the experimental setup.

The third enzyme to be examined in this section is endonuclease III-

Single-base lesions

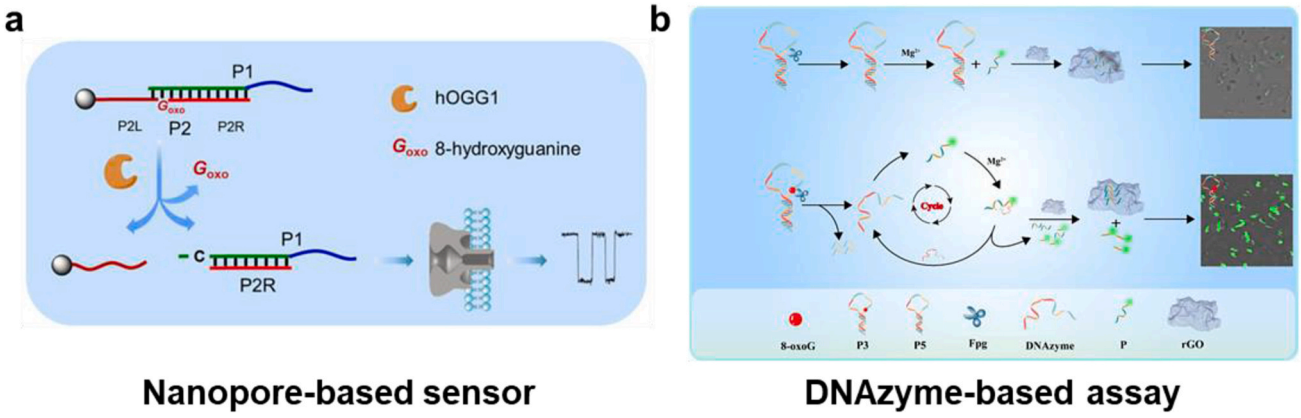

* FRET: Fluorescence Resonance Energy Transfer

Bulky adducts or crosslinks

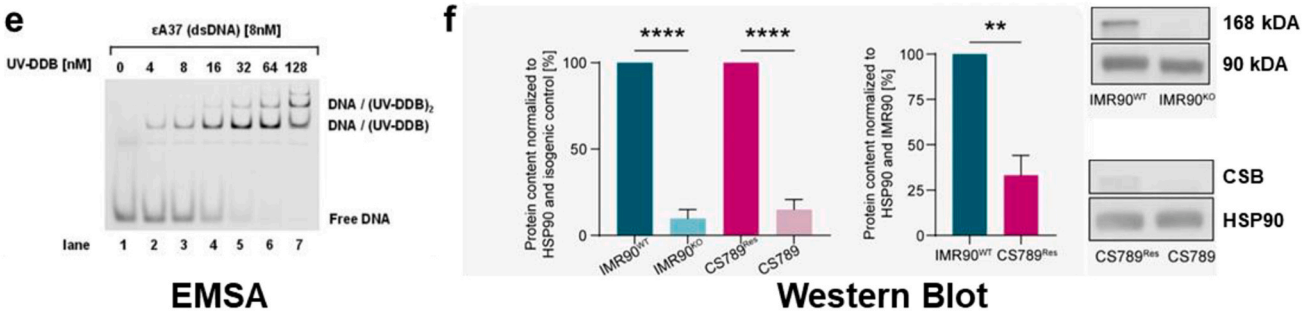

* EMSA: Electrophoretic Mobility Shift Assay

Double-strand break

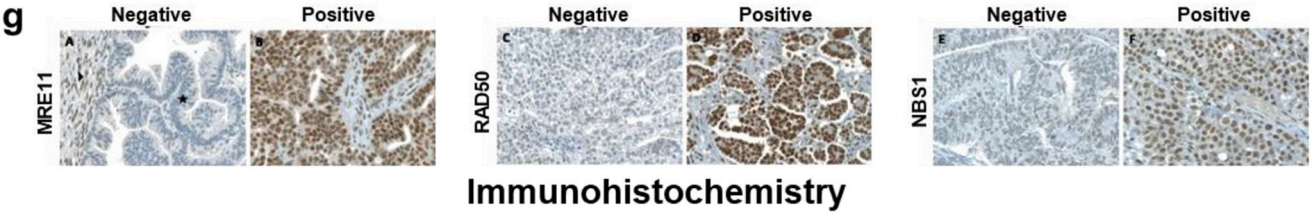

(caption on next page)

Fig. 3. Measurements of DNA repair enzymes. (a–d) Detection of enzymes involved in BER. (a) Detected hOGG1 activity using a nanopore-based sensor, which measures current blockades as DNA fragments pass through an α-hemolysin nanopore. Reproduced with permission from ref. [69]. (b) Measured FPG activity using a DNAzyme-based assay with rGO quenching. Reproduced with permission from ref. [73]. (c) Detected AAG activity using a quantum dot FRET nanosensor with a hairpin-structured detection probe. Reproduced with permission from ref. [82]. (d) Detected APE1 activity using a DNA structure-mediated fluorescent biosensor with dual signal amplification. Reproduced with permission from ref. [85]. (e–f) Detected enzymes involved in NER. (e) Detected UV-DDB binding to DNA lesions using EMSA, visualized via fluorescence scanner. Reproduced with permission from ref. [80]. (f) Quantified CSB protein levels in hiPSC-derived neural progenitor cells using Western blot and normalized against HSP90. Reproduced with permission from ref. [93]. (g) Detected enzymes involved in DSB repair. MRN complex (MRE11, RAD50, and NBS1) detected in ovarian carcinoma samples using IHC) and scored based on nuclear staining intensity. Reproduced with permission from ref. [102]. FPG, formamidopyrimidine glycosylase; rGO, reduced graphene oxide; AAG, alkyladenine DNA glycosylase; FRET, Förster resonance energy transfer; APE1, apyrimidinic endonuclease 1; UV-DDB, UV-damaged DNA-binding; EMSA, electrophoretic mobility shift assay; CSB, Cockayne syndrome group B; IHC, immunohistochemistry.

Table 3
Comparative table of DNA damage detection methods.

Method	Sensitivity	Advantages	Limitations
Comet Assay	Moderate (0.1–10 lesions)	- Low cost - Versatile	- Labor intensive - Semi-quantitative
HPLC-ECD	High (nM range)	- Quantitative for oxidative lesions	- Limited to redox-active lesion - Requires special equipment
LC-MS/MS	Ultra-high (fM range)	- Detects multiple lesion types	- Expensive instrumentation - Complex data analysis
qPCR	High (1 lesions/10^4-10^6bp)	- Gene-specific damage analysis - Cost effective	- Limited to amplified region - Primer design challenges
Immunological Assay (ex - ELISA)	Moderate-High (pM range)	- High-throughput - Lesion-specific	- Antibody cross-reactivity - Limited to pre-characterized spot
Flow Cytometry (γH2AX foci)	Moderate	- Single-cell resolution	- Requires fluorescence labeling - Limited to DSBs
CRISPR-based detection	Ultra-high (single-molecule)	- Single-nucleotide resolution - Programmable for any locus	- Technically complex - Off-target effects possible
NGS	Ultra-high	- Genome-wide lesion mapping - Identifies mutation spectra	- High cost - Computationally intensive
Live-Cell Imaging	Moderate	- Real-time - Dynamic repair kinetics	- Low throughput - Requires fluorescent probes

like protein 1 (NTHL1), which is responsible for identifying and excising thymine glycol lesions [74]. Alekseeva et al. developed specific DNA probes containing thymine glycol, which are tagged with a fluorescent molecule and a quencher at both ends, forming a Förster resonance energy transfer (FRET) system [75]. Upon cleavage of these probes by NTHL1, the fluorescence signal increases, allowing for quantification of the enzyme activity. The method is highly sensitive and scalable, however, detecting in complex biological samples may be limited owing to potential interference.

Uracil-DNA glycosylase (UDG) is the enzyme that recognizes and removes uracil from DNA, excising the base by cleaving the glycosidic bond between uracil and the sugar-phosphate DNA backbone [76]. Lu et al. introduced a luminescent switch-on assay for detecting UDG activity [77]. The method utilizes a DNA duplex substrate containing a lesion paired with a complementary strand capable of forming a G-quadruplex structure. Upon uracil excision by UDG, the complementary strand is released to form a G-quadruplex. The structural shift is then detected by a novel fluorescent probe, DID-VP, a newly developed charged organic molecule that specifically binds to the G-quadruplex, resulting in a significant fluorescence increase. The method detects UDG activity with high sensitivity, achieving a detection limit of 0.005 U/mL, and demonstrates high specificity. However, DID-VP probe synthesis and potential background fluorescence present limitations. Squillaro et al. employed quantitative PCR (qPCR) for detecting and quantifying UDG activity [78]. The approach involves preparing DNA substrates containing uracil bases by amplifying a specific DNA region with PCR, incorporating deoxyuridine triphosphate (dUTP) instead of thymidine triphosphate (dTTP). The DNA substrates are then incubated with cell or tissue extracts containing active UDG, resulting in enzyme cleaving to uracil bases. This cleavage reduces PCR amplicon yield, which is subsequently quantified using qPCR. The assay provides precise quantification without requiring radiolabeled substrates and relies on a reliable, relatively simple technique. However, its indirect nature and dependency on the PCR step present limitations.

Hypoxanthine is recognized and excised by alkyladenine DNA glycosylase (AAG) [79,80]. Wang et al. presented a fluorescence-based method for AAG activity detection using a target-mediated hyperbranched signal amplification process [81]. When AAG excises damaged DNA bases, the enzyme Endonuclease IV (Endo IV) creates nicked sites, which Terminal deoxynucleotidyl transferase (TdT) extends by adding nucleotides to the 3′ ends, resulting in the formation of hyperbranched DNA structures. A fluorescent dye specifically binds to these branched structures, generating a fluorescent signal that correlates with AAG activity. This method is highly sensitive, with a detection limit of 0.090 U/mL, and is simple to apply, requiring no comprehensive steps such as immobilization or washing. However, it relies on precise specialized reagent preparation and accurate fluorescence measurement, which may limit its accessibility and require high-quality instrumentation. Liu et al. developed a fluorescence-based method for detecting AAG activity using a quantum dot (QD) FRET nanosensor (Fig. 3c) [82]. The technique employs a single hairpin-structured detection probe containing a deoxyinosine (I) base, which AAG specifically excises, generating an AP site. This site is further processed by APE1, forming a 3′-OH terminus that initiates a strand displacement reaction. This reaction generates multiple single-stranded DNA (ssDNA) signal probes that self-assemble on the QD surface, facilitating efficient FRET between the QD and a Cy5 fluorophore on the ssDNA, producing a fluorescent signal. The method offers high sensitivity, with a detection limit of 3.60×10^{-10} U/μL, and is simple, using a single probe for both sensing and signal amplification. However, it requires precise probe preparation and accurate fluorescence measurement, which may necessitate specialized equipment. Zhang et al. developed a fluorescence-based method using BER-mediated cascading triple-signal amplification [83]. The method begins with AAG excising deoxyinosine from a DNA substrate, creating an AP site, which Endo IV then cleaves the DNA to initiate an SDA reaction. The resulting SDA-generated primers bind to a circular template, initiating primer generation rolling circle amplification (PG-RCA) and producing numerous primers. These primers then cleave signal probes, generating an amplified fluorescence signal. The method is highly sensitive, with a detection limit of 0.026 U/mL, and simplifies the process by eliminating complex steps such as immobilization. However, it requires precise control over amplification to maintain specificity and prevent nonspecific signal amplification.

AP sites can arise from external factors or through glycosylase action

during BER. These lesions require further processing, starting with recognition and cleavage by apurinic/apyrimidinic endonuclease 1 (APE1) [84]. Fig. 3d illustrates a fluorescent biosensor for detecting APE1 activity developed by Hu et al. using a DNA structure-mediated approach with dual signal amplification [85]. The method employs a hairpin DNA substrate containing an AP site and a 3′-NH2 group to prevent background signal generation. Upon APE1 cleavage, the AP site forms a 3′-OH terminus, prompting TdT to elongate a poly-adenine tail. This tail then hybridizes with multiple poly-thymine probes containing fluorophores and quenchers. Subsequent Endo IV cleavage releases the fluorophores from quenchers, generating a fluorescence signal. With a detection limit of 1.7×10^{-6} U/mL, the method is highly sensitive for APE1 detection assays. However, it requires precise substrate design and careful amplification step control, limiting its applicability in less controlled environments. Li et al. developed a label-free fluorescence-based method for detecting APE1 activity using an AP site-binding fluorophore, 2-amino-5,6,7-trimethyl-1,8-naphthyridine (ATMND) [86]. The method uses a DNA duplex containing an AP site analog, where ATMND fluorescence is quenched upon binding to the AP site. Cleavage of the AP site by APE1 releases ATMND, resulting in fluorescence recovery. These fluorescence changes directly correlate with APE1 activity, enabling its quantification. With a detection limit of 0.04 U/mL, the method is sensitive, advantageous owing to its simplicity, and eliminates the need for labeled probes. However, its effectiveness relies on precise control of experimental conditions to ensure accurate detection.

3.2. Measurement of markers involved in NER pathway

The NER pathway is a crucial DNA repair mechanism that maintains genomic stability by removing various DNA lesions, such as CPDs and 6-4 PPs, as discussed in the previous section [87]. It consists of two sub-pathways: Global Genome NER (GG-NER), which scans the entire genome for damage, and Transcription-Coupled NER (TC-NER), which targets repairing lesions that block transcription by stalling RNA polymerase II in actively expressed genes [88].

In the GG-NER pathway, the UV-damaged DNA-binding protein complex (UV-DDB) is crucial for recognizing CPDs and 6-4 PPs. This protein, composed of DDB1 and DDB2 proteins, has a high affinity for UV-induced lesions [89,90]. Jang et al. used an Electrophoretic Mobility Shift Assay (EMSA) to detect and quantify UV-DDB binding to specific lesion-containing DNA substrates [80]. (Fig. 3e) The method utilized a fluorescein-labeled DNA duplex with a modified base. UV-DDB binding to these substrates was analyzed by incubating increasing UV-DDB concentrations with labeled DNA and running the mixtures on a native polyacrylamide gel. UV-DDB binding to the damaged DNA alters DNA band migration, visualized using a fluorescence scanner. The degree of shift indicates the binding affinity of UV-DDB for the lesion-containing DNA. The assay confirmed strong binding UV-DDB preference for damaged DNA over undamaged DNA, with calculated dissociation constants (Kd) indicating high affinity. These gel mobility shifts directly correlate with UV-DDB binding, providing a quantitative measurement of UV-DDB activity and interaction with DNA lesions. The EMSA method is highly sensitive, allowing precise quantification of binding characteristics of UV-DDB to various DNA lesions, though direct quantification remains limited. Fei et al. quantified cellular UV-DDB levels using chromatin digestion assay followed by Western blotting to detect the DDB2 subunit, a component of UV-DDB. After UV irradiation, the chromatin was treated with micrococcal nuclease (MNase) to selectively digest internucleosomal linker DNA, isolating solubilized internucleosomal sites from insoluble core particles [91]. Quantification revealed approximately 70 % of DDB2 in the solubilized fraction and 20 % in core particles. This method enables precise UV-DDB localization and quantification in chromatin structures but excludes DDB1, requires careful control of MNase digestion conditions, and relies on antibody specificity, introducing variability in the results.

In the TC-NER pathway, Cockayne syndrome group B (CSB) protein is essential for recognizing stalled RNA polymerase II at pyrimidine dimer sites and initiating the repair process [92]. Kapr et al. quantified CSB protein levels in hiPSC-derived neural progenitor cell (hiNPC) neurospheres using Western blot analysis (Fig. 3f) [93]. CSB was detected with specific antibodies, and chemiluminescence was employed to visualize the bands. The signal intensity of the CSB bands was measured and normalized to the loading control (HSP90) for accuracy. Western blot is widely used for detecting specific proteins owing to its sensitivity and specificity; however, it has limitations related to reproducibility, method reporting, and result accuracy [94]. Lindsey-Boltz et al. employed Quantitative Excision Repair Sequencing (qXR-Seq) to assess DNA repair activity as an indirect quantification of functional CSB in human cell lines [95]. This method involved spiking a known quantity of UV-irradiated Drosophila DNA as an internal standard into human cell lysates, followed by the detection of excised DNA oligonucleotides from NER activity. Comparing the ratio of human to Drosophila excision products enabled the quantification of relative excision repair efficiency across various cell lines. qXR-Seq data revealed a significantly reduced level of repair activity in XPC−/−/CSB−/− double knockout cells, approximately 0.3 % of observed wild-type cell activity, underscoring the critical role of CSB in maintaining DNA repair. While highly sensitive and quantitative, this method relies on the accurate calibration of the internal standard and it may be influenced by biological sample complexity.

3.3. Measurement of markers involved in DSB repair pathway

The DSB repair pathway relies on two primary mechanisms by which cells repair DSBs— non-homologous end joining (NHEJ) and homology-directed repair (HDR) [96,97]. Each pathway relies on specific protein complexes to recognize and initiate repair at the DNA damage site. In the NHEJ pathway, the Ku heterodimer (comprising Ku70 and Ku80) binds and stabilizes broken DNA ends, recruiting additional proteins needed for direct ligation of the ends without requiring a homologous template. Conversely, in the HDR pathway, the MRN complex (comprising MRE11, RAD50, and NBS1) is crucial for recognizing DSBs, processing DNA ends to generate 3′ single-stranded overhangs, and recruiting factors for repair using a sister chromatid or homologous chromosome as a template to accurately restore the original DNA sequence [98,99]. Various methods are used to detect these proteins.

Lee et al. developed a method to analyze Ku heterodimer (Ku70/Ku80) dissociation from DNA ends using biochemical and fluorescence-based assays [100]. The method involves the use of *in vitro* pull-down assays with biotinylated forked double-stranded DNA (dsDNA) bound by Ku heterodimer. Phosphorylation of Ku70 by DNA-PKcs (DNA-dependent protein kinase catalytic subunit) in the presence of ATP induces a structural shift, causing it to detach from the DNA. Dissociation is then quantified by measuring the Ku70 remaining bound to the dsDNA vs. that released into the supernatant, using Western blot analysis. Additionally, the researchers employed fluorescence recovery after photobleaching (FRAP) and live-cell imaging to observe Ku70 dynamics at DNA damage sites, providing real-time assessment of Ku heterodimer behavior in cells. This approach allowed the authors to correlate the phosphorylation state of Ku70 with its DNA-binding affinity, revealing that Ku70 phosphorylation decreases its affinity for DNA, facilitating its release and enabling DNA end resection—a crucial step in the homologous recombination repair pathway. The method effectively elucidates the mechanism underlying DNA repair pathway selection and is sensitive to Ku70 phosphorylation status. Mukherjee et al. measured the Ku heterodimer using a combination of Western blot analysis and kinase assays with Western blot [101]. In the Western blot analysis, Ku70 and Ku80 proteins were detected with specific antibodies to quantify Ku heterodimer levels under various experimental conditions, assessing protein amounts based on band intensity on the blot. In the kinase assays with Western blot, Ku70 served as a substrate to examine its

phosphorylation by various cyclin-dependent kinases (Cdks). Phosphorylated Ku70 was separated via SDS-PAGE and visualized with a phosphorimager, enabling the quantification of the phosphorylated Ku70 and providing insights into its effects on Ku heterodimer function in DNA repair and replication. However, this method shares the limitations mentioned in Section 3.2.

Brandt et al. analyzed the MRN complex in a tissue microarray (TMA) composed of 134 ovarian carcinoma samples using immunohistochemistry (IHC) [102]. In this method, specific antibodies were used to detect the presence of MRE11, RAD50, and NBS1 proteins, the components of the MRN complex (Fig. 3g). Nuclear staining intensity in tissue sections was evaluated and scored from negative (0) to strong (3) to quantify protein levels of the MRN complex. This approach enabled the researchers to determine MRN complex deficiency prevalence in ovarian cancer and its correlation with different clinicopathological features and potential sensitivity to poly (ADP-ribose) polymerase (PARP) inhibitors. IHC is advantageous for visualizing protein localization and expression levels directly within tissue samples, but it is semi-quantitative and subject to variability in antibody specificity and staining conditions [103]. Matsuda et al. quantified the MRN complex components—MRE11, RAD50, and NBS1 in EPC2-hTERT cells using liquid chromatography-tandem mass spectrometry (LC-MS/MS), allowing precise molecular-level measurement [104]. The absolute quantities were determined as 6.89×10^4 molecules per cell for MRE11, 2.17×10^4 for RAD50, and 2.35×10^4 for NBS1. MRN complex protein abundance is crucial for detecting and repairing DNA DSB. LC-MS/MS offers high sensitivity and precise protein quantification but requires extensive sample preparation and can be limited by specific internal standard availability [105].

3.4. Limitations arising from repair pathway characteristics

While Chapter 2 focuses on the direct measurement of DNA damage, Chapter 3 measures proteins expressed in response to damage, leading to certain limitations due to the nature of this approach. For instance, while FPG is commonly used to detect FapyG lesions, many FPG detection methods depend on 8-OHdG as a substrate, which raises concerns regarding specificity for FapyG lesions [106]. Similarly, deoxyinosine is typically used to identify AAG, but this approach may not be optimal for detecting hypoxanthine lesions [107]. At present, glycosylases are widely used as biomarkers for single-base lesion repair owing to their dual functions in recognition and cleavage, enabling the development of highly sensitive and accurate detection methods [108]. However, enzymes involved in NER and DSB repair pathways lack these dual characteristics, limiting their effectiveness in precise quantification. Therefore, overcoming the inherent limitations of these DNA repair mechanisms is crucial for improving detection accuracy and advancing DNA damage analysis.

4. Clinical applications of DNA damage detection

DNA damage detection technologies play a crucial role in clinical settings by offering several significant advantages, particularly in observing patients' health at the genetic level. First and foremost, early detection of DNA damage can help prevent disease progression in conditions such as cancer, allowing patients to avoid expensive and painful surgeries. Moreover, given the heterogeneous nature of human beings, personalized medicine has become increasingly important. By analyzing a patient's unique genetic makeup and specific patterns of DNA damage, healthcare providers can tailor treatment strategies to individual patients. Additionally, if these technologies are utilized for monitoring treatment responses and assessing prognosis, clinicians can evaluate the effectiveness of therapies and make necessary adjustments to treatment plans. As such, DNA damage detection techniques can be critically important in clinical settings. This chapter aims to introduce how DNA damage detection can be applied in cancer diagnostics, personalized medicine, aging and age-related diseases, and monitoring treatment efficacy (Fig. 4).

4.1. Cancer diagnostics

Early detection and effective management of cancer progression play a critical role in enhancing treatment outcomes and improving patient survival [109,110]. In this context, understanding and detecting DNA lesions—as well as the repair mechanisms that safeguard genomic integrity—is essential because disruptions in these pathways can lead to genomic instability, a hallmark of cancer that predisposes cells to malignant transformation and rapid disease progression [111]. By providing insights into genomic instability, DNA repair deficiencies, and specific biomarkers associated with cancer development, these techniques have opened new avenues for early cancer diagnosis and intervention.

There are several markers for cancer detection such as γH2AX and Ku70/Ku80. γH2AX can be utilized not only to identify genetic effects caused by various toxic agents but also to assess the clinical efficacy of chemotherapy and radiotherapy, as well as the changes in sensitivity of cancer cells to anticancer drugs [112]. Furthermore, screening for the functional variants of H2AX and targeting H2AX have been proposed as potential cancer treatments [113]. The expression of Ku70/Ku80 has also shown a significant increase in rectal cancer patients following chemotherapy and radiotherapy, with further studies indicating that this increase is associated with chemo- and radio-resistance in various cancers [114]. However, these DNA damage response (DDR) sensors are still in the early stages of molecular characterization, and their roles in detecting DNA damage, signaling, cancer progression, and therapy require further investigation [5].

Detecting deficiencies in repair pathways and assessing genomic instability are also important strategies for early cancer diagnosis. The detection of mismatch repair (MMR) deficiency has become crucial in screening for colorectal, gastric, endometrial, and ovarian cancers [111]. Defects in the DNA MMR proteins lead to a phenotype known as microsatellite instability (MSI), which occurs in up to 15 % of sporadic colorectal cancers [115]. Identifying tumors with deficient MMR is essential for cancer screening, particularly for Lynch syndrome, as it not only informs treatment decisions but also allows at-risk family members to undergo appropriate screening and monitoring. Park et al. utilized five microsatellites (BAT-26, BAT-25, D5S346, D2S123, and D17S250) for PCR-based MSI testing, highlighting the significance of MMR deficiency detection in screening for gastric cancer [116].

4.2. Targeted therapy and treatment efficacy monitoring

As explained in previous chapter, DNA damage detection technologies, such as γH2AX and comet assays, hold significant potential for advancing personalized medicine. These assays enable the quantification of individual DNA damage responses, which can guide tailored cancer therapies by predicting patient-specific radiosensitivity or chemosensitivity, as well as monitoring treatment efficacy and minimizing adverse effects [117]. This understanding of tumor heterogeneity and individual treatment responses has facilitated the identification of adequate biomarkers. However, there remains a need to demonstrate that the level of automation and standardization of these technologies is sufficient for assessment in clinical studies.

Another important substance in targeted therapy development is PARP inhibitors (PARPi) [118]. PARPi exploit synthetic lethality in tumor cells with homologous recombination deficiencies, such as BRCA1/2 mutations, by preventing efficient DNA repair. This leads to the accumulation of DNA damage, ultimately triggering tumor cell death while sparing normal cells. The success of PARP inhibitors, including olaparib, rucaparib, and niraparib, in treating cancers such as BRCA-mutated breast, ovarian, and prostate cancers underscores the critical role of DNA damage detection in identifying suitable candidates

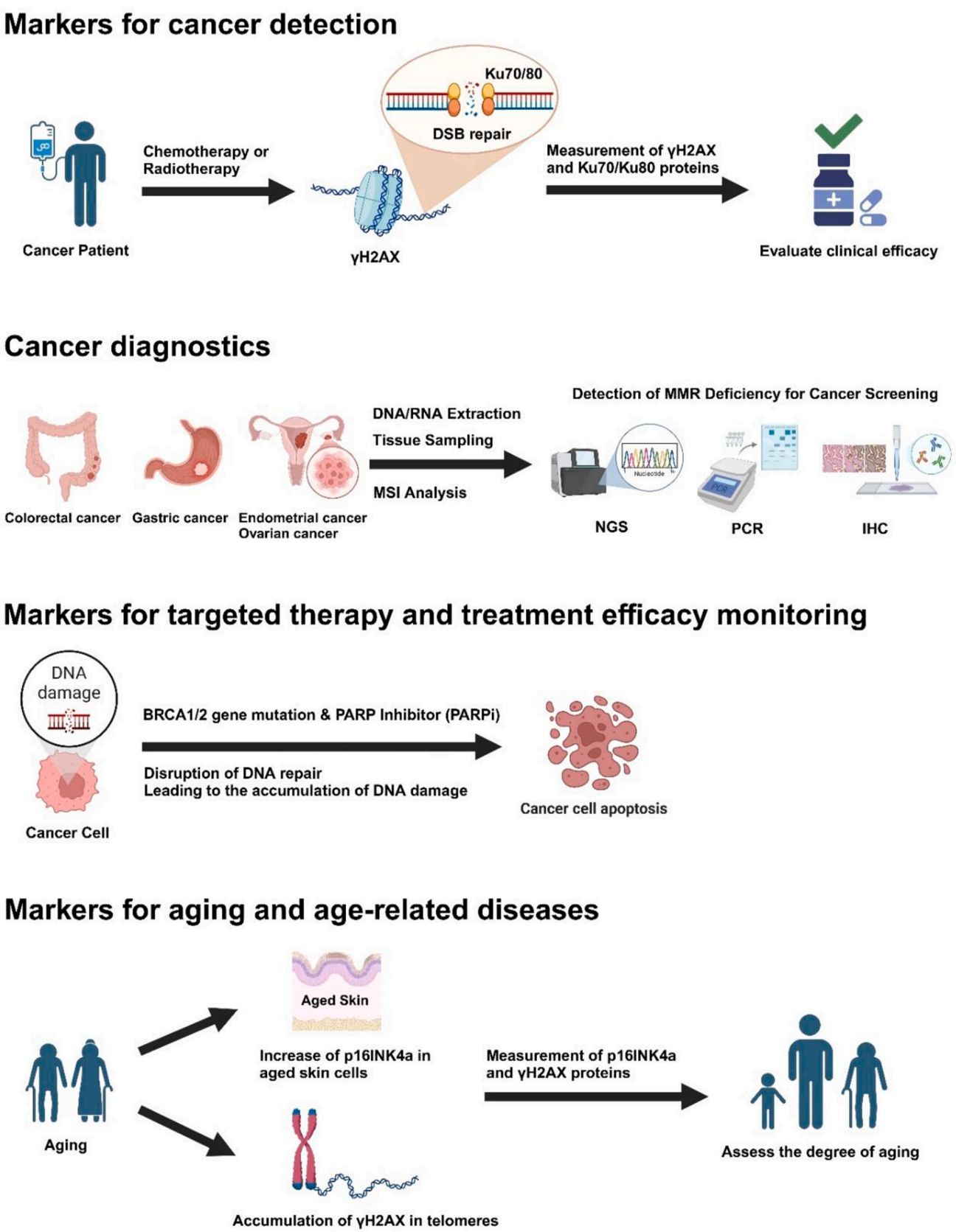

Fig. 4. DNA damage detection technologies and biomarkers in clinical applications. Current applications encompass cancer diagnostics, targeted therapy, treatment efficacy monitoring, and aging research. γH2AX and Ku70/Ku80 are key markers for evaluating treatment efficacy in cancer patients, while PARP inhibitors play a crucial role in targeted therapy development. Additionally, γH2AX and p16INK4a are used to assess aging. These biomarkers are essential for cancer diagnostics, personalized treatment strategies, and understanding age-related diseases, underscoring the importance of DNA damage detection in disease prevention and therapeutic monitoring.

for these therapies.

4.3. Aging and age-related diseases

DNA damage detection techniques not only address severe diseases like cancer but also reveal the central role of genomic instability in aging and age-related diseases. Key biomarkers of aging include γH2AX and p16INK4a. Numerous studies have shown that γH2AX accumulates with age, particularly in telomeric DNA and in cells undergoing cellular senescence [49,119,120]. Additionally, elevated levels of endogenous γH2AX have been linked to diseases associated with accelerated aging [49]. While γH2AX is a promising biomarker for aging, it has various applications and should be considered alongside other markers and factors when studying the aging process. The expression of p16INK4a is a result of chemotherapy-induced DNA damage. Ressler et al. found that the number of p16INK4a-positive cells is significantly higher in elderly individuals compared to younger age groups, both in the epidermis and dermis, indicating that p16INK4a expression directly correlates with chronological aging in human skin [121]. Liu et al. discovered that in adolescents and young adults undergoing chemotherapy, significant increases in p16INK4a expression were associated with frailty, representing a 35-year acceleration in biological age among frail young adult cancer survivors, particularly in peripheral T cells [122]. These findings demonstrate that p16INK4a expression serves as a biomarker of cellular and organismal aging across different tissues and species. Moreover, it not only correlates with chronological age but also reflects the influence of lifestyle factors and environmental stressors on biological aging.

DNA damage detection techniques are not only beneficial for studying aging but also for investigating various age-related diseases, including cancer, neurodegenerative diseases, cardiovascular disease, and premature aging syndromes. These disorders are associated with DNA repair deficiencies, such as mutations and microsatellite instability —a marker of defective mismatch repair—as well as the accumulation of DNA damage [123–125]. Therefore, effective detection technologies for these issues can open new avenues for potential interventions aimed at promoting healthy aging.

5. Discussion

This review comprehensively outlines DNA damage and repair mechanisms, along with various methods for measuring associated biomarkers. While DNA damage assessment primarily targets physical and chemical change detection in the DNA, DNA repair measurement focuses on detecting enzymatic activities using biosensors, fluorescence, and immunoassays. These techniques provide valuable insights into the response to DNA damage in the body rather than the damage itself.

DNA damage detection methods have significantly evolved over time (Fig. 5). Initially, commonly used techniques included the comet assay, single HPLC or MS, and Western blot. However, these methods had limitations, including low sensitivity, specificity, and being labor-intensive. Subsequently, combined methods like HPLC-ECD and LC-MS/MS emerged. The incorporation of electrochemical detection on HPLC greatly enhanced sensitivity for oxidative DNA lesions, such as 8-oxoG, and allowed for the selective detection of a wide range of oxidative stress markers in biological samples, including urine, plasma, and DNA extracts. LC-MS/MS integrates the separation capabilities of liquid chromatography with the high sensitivity and specificity of tandem mass spectrometry, enabling the detection of DNA lesions at femtomolar concentrations and the differentiation between structurally similar adducts, such as 8-oxoG and other guanine derivatives.

In addition to these improvements in sensitivity and specificity, advances such as the introduction of the qPCR have facilitated not only qualitative but also quantitative assessments of DNA damage. Furthermore, qPCR can be performed in a high-throughput format using 96-well or 384-well plates, enabling the simultaneous analysis of multiple samples. This flexibility makes qPCR suitable for both small-scale studies, such as single-gene analyses, and large-scale applications, including genome-wide assessments when combined with techniques like next-generation sequencing (NGS) [126].

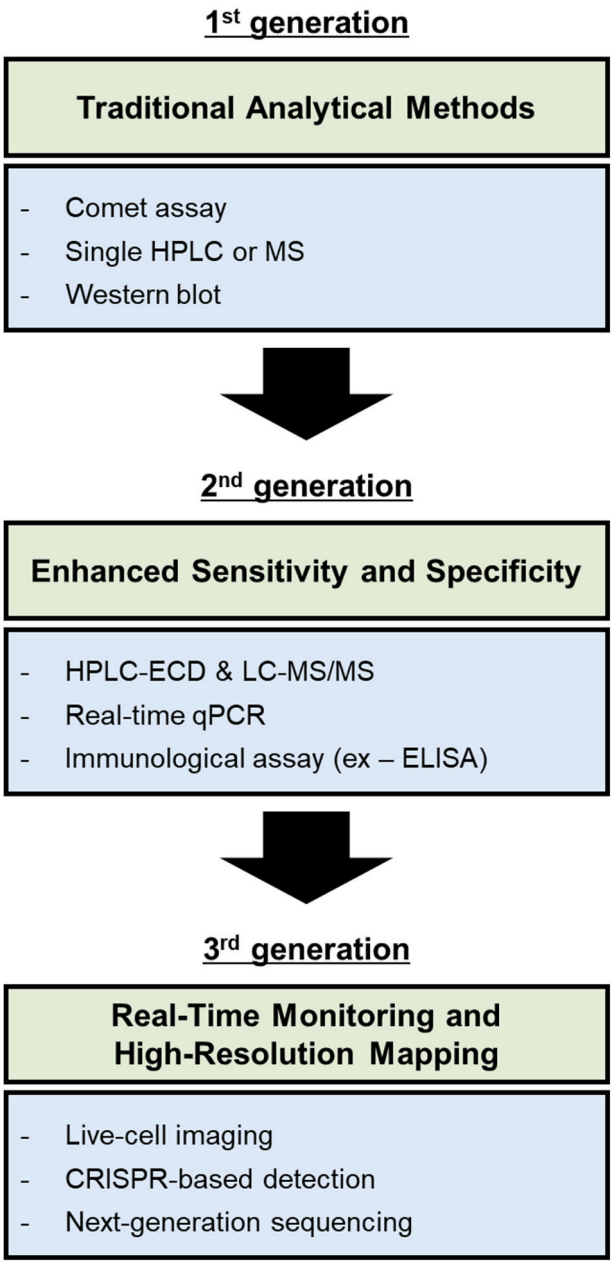

Fig. 5. Flowchart illustrating the evolution of DNA damage detection methods from 1st generation to 3rd generation. The progression demonstrates advancements from foundational techniques with moderate sensitivity and specificity to methods offering significant improvements in detection accuracy. The 3rd generation introduces high-resolution mapping, real-time monitoring of repair processes, and genome-wide lesion profiling, highlighting the increasing sophistication and versatility of DNA damage detection technologies over time.

Achieving high sensitivity and specificity is essential, but the next frontier lies in real-time monitoring and high-resolution mapping, which are vital for advancing our understanding of DNA damage. Real-time monitoring effectively captures dynamic processes, providing insights into DNA repair pathways and drug treatment efficacy [127]. While fluorescent protein-based sensors have advanced the visualization of DNA damage responses in living cells, they often rely on indirect damage markers (such as repair protein recruitment) rather than direct DNA lesion detection [44,128]. The development of live-cell imaging

technologies and biosensors that directly monitor DNA damage and repair in real time could significantly enhance our understanding of cellular responses to environmental stressors and advance DNA repair studies. Meanwhile, high-resolution mapping allows researchers to precisely identify the genomic locations of DNA lesions and connect this damage to functional consequences, facilitating the exploration of how such damage impacts gene expression, chromatin structure, and overall cellular function [129,130].

Complementing these experimental advances, AI and machine learning algorithms—widely employed in disease diagnosis—are increasingly being applied to predict repair pathway choices and to quantify DNA damage in high-throughput assays [131–133]. These technologies are not only refining our mechanistic understanding of DNA repair processes but also uncovering novel genetic interactions and potential synthetic lethalities that could be exploited for targeted cancer therapies.

The development of DNA damage detection techniques has led to fundamental discoveries in DNA repair mechanisms. For example, early HPLC combined with radiolabeling techniques enabled the identification of AP sites in E. coli exposed to alkylating agents, which directly contributed to the discovery of the BER pathway [134]. Additionally, this approach played a key role in identifying DNA glycosylases such as OGG1, which is critical for removing 8-oxoG, an oxidative lesion linked to cancer and aging [135]. These early chromatographic and biochemical techniques laid the groundwork for understanding the enzymatic mechanisms of DNA repair.

In addition, the technological advancements have also profoundly enhanced our understanding of cellular processes and disease mechanisms. For instance, live-cell imaging of repair proteins, such as fluorescently tagged RAD51, has further demonstrated how repair pathway activation is dynamically regulated by cell cycle phase and chromatin context [136]. Similarly, mass spectrometry-based quantification of oxidative lesions has linked oxidative DNA damage to mitochondrial dysfunction and neurodegenerative diseases, such as Alzheimer's and Parkinson's disease [137]. Furthermore, qPCR and the comet assay have been instrumental in diagnosing inherited repair disorders, such as xeroderma pigmentosum and Lynch syndrome, by confirming defects in NER and mismatch repair, respectively [138,139]. In cancer research, genome-wide CRISPR screens and NGS have uncovered synthetic lethality between PARP inhibitors and BRCA1/2 mutations, leading to the development of FDA-approved therapies for HR-deficient cancers.

Based on these advanced technologies, future research is focusing on developing more sensitive and clinically translatable diagnostics. NGS techniques and sensor-based platforms are being adapted for real-time, in situ monitoring of DNA lesions. At the same time, CRISPR-based biosensors and wearable devices are expanding the toolkit for rapid, non-invasive detection of damage biomarkers in clinical settings. Moreover, the integration of multi-omics approaches—including single-cell sequencing, spatial transcriptomics, and proteogenomics—will enable a more comprehensive profiling of repair pathway heterogeneity across various tissues and disease states. This would be helpful for understanding variations in individual genetic profiles and treatment responses that are essential for developing effective, personalized therapies [140]. As these emerging methods continue to mature, standardizing protocols and establishing ethical frameworks will be crucial for their widespread adoption, ultimately bridging the gap between bench research and precision medicine in the management of genomic instability. Also, this approach could enhance effective disease profiling and biomarker discovery, further advancing the fields of personalized healthcare, particularly for aging populations and space medicine.

CRediT authorship contribution statement

Heeseok Kang: Writing – review & editing, Writing – original draft, Conceptualization. **Hyung Joon Park:** Writing – review & editing, Writing – original draft, Conceptualization. **Jieun Kang:** Writing – review & editing, Writing – original draft, Conceptualization. **Yuna Hwang:** Investigation. **YongJin Lee:** Investigation. **Sang-Uk Park:** Investigation. **Jeongkyu Kim:** Supervision, Funding acquisition, Conceptualization. **Kwan Hyi Lee:** Supervision, Funding acquisition, Conceptualization. **Sunbok Jang:** Writing – review & editing, Supervision, Funding acquisition, Conceptualization.

Declaration of competing interest

The authors declare that they have no known competing financial interests or personal relationships that could have appeared to influence the work reported in this paper.

Acknowledgments

This work was supported by the National Research Foundation of Korea grant funded by the Korean government (MSIT) (Grant Numbers: RS-2025-00523062, 2022R1F1A1068560 and RS-2023-00217701) and Chung-Ang University Research Scholarship Grants in 2021. This work was also supported by the Korea Institute of Science and Technology (KIST) Institutional program (2E33741), the Nanomedical Devices Development Project of the NNFC in 2025, and the KU-KIST Graduate School of Converging Science and Technology, Korea University (2V10331).

Data availability

Data will be made available on request.

References

[1] N.Z. Lax, D.M. Turnbull, A.K. Reeve, Mitochondrial mutations: newly discovered players in neuronal degeneration, Neuroscientist 17 (2011) 645–658, https://doi.org/10.1177/1073858410385469.

[2] Y. Zong, H. Li, P. Liao, L. Chen, Y. Pan, Y. Zheng, C. Zhang, D. Liu, M. Zheng, J. Gao, Mitochondrial dysfunction: mechanisms and advances in therapy, Signal Transduct. Targeted Ther. 9 (2024) 124, https://doi.org/10.1038/s41392-024-01839-8.

[3] S.-J. Kim, P. Cheresh, M. Eren, R.P. Jablonski, A. Yeldandi, K.M. Ridge, G.R. S. Budinger, D.-H. Kim, M. Wolf, D.E. Vaughan, D.W. Kamp, Klotho, an antiaging molecule, attenuates oxidant-induced alveolar epithelial cell mtDNA damage and apoptosis, Am. J. Physiol. Lung Cell. Mol. Physiol. 313 (2017) L16–L26, https://doi.org/10.1152/ajplung.00063.2017.

[4] B. Schumacher, J. Pothof, J. Vijg, J.H.J. Hoeijmakers, The central role of DNA damage in the ageing process, Nature 592 (2021) 695–703, https://doi.org/10.1038/s41586-021-03307-7.

[5] R. Huang, P.-K. Zhou, DNA damage repair: historical perspectives, mechanistic pathways and clinical translation for targeted cancer therapy, Signal Transduct. Targeted Ther. 6 (2021) 254, https://doi.org/10.1038/s41392-021-00648-7.

[6] M. Jiang, K. Jia, L. Wang, W. Li, B. Chen, Y. Liu, H. Wang, S. Zhao, Y. He, C. Zhou, Alterations of DNA damage response pathway: biomarker and therapeutic strategy for cancer immunotherapy, Acta Pharm. Sin. B 11 (2021) 2983–2994, https://doi.org/10.1016/j.apsb.2021.01.003.

[7] C. Toader, N. Dobrin, F.-M. Brehar, C. Popa, R.-A. Covache-Busuioc, L.A. Glavan, H.P. Costin, B.-G. Bratu, A.D. Corlatescu, A.A. Popa, A.V. Ciurea, From recognition to remedy: the significance of biomarkers in neurodegenerative disease pathology, Int. J. Mol. Sci. 24 (2023) 16119, https://doi.org/10.3390/ijms242216119.

[8] R.E. Connon, J. Geist, I. Werner, Effect-based tools for monitoring and predicting the ecotoxicological effects of chemicals in the aquatic environment, Sensors (Basel) 12 (2012) 12741–12771, https://doi.org/10.3390/s120912741.

[9] M. Moreno-Villanueva, M. Wong, T. Lu, Y. Zhang, H. Wu, Interplay of space radiation and microgravity in DNA damage and DNA damage response, NPJ Microgravity 3 (2017) 14, https://doi.org/10.1038/s41526-017-0019-7.

[10] E. Pariset, A. Bertucci, M. Petay, S. Malkani, A. Lopez Macha, I.G. Paulino Lima, V. Gomez Gonzalez, A.S. Tin, J. Tang, I. Plante, E. Cekanaviciute, M. Vazquez, S. V. Costes, DNA damage baseline predicts resilience to space radiation and radiotherapy, Cell Rep. 33 (2020) 108434, https://doi.org/10.1016/j.celrep.2020.108434.

[11] A. Kingsland, L. Maibaum, DNA base pair mismatches induce structural changes and alter the free-energy landscape of base flip, J. Phys. Chem. B 122 (2018) 12251–12259, https://doi.org/10.1021/acs.jpcb.8b06007.

[12] L.-J. Mah, A. El-Osta, T.C. Karagiannis, gammaH2AX: a sensitive molecular marker of DNA damage and repair, Leukemia 24 (2010) 679–686, https://doi.org/10.1038/leu.2010.6.

[13] J.P. Kehrer, Free radicals as mediators of tissue injury and disease, Crit. Rev. Toxicol. 23 (1993) 21–48, https://doi.org/10.3109/10408449309104073.

[14] M. Valko, M. Izakovic, M. Mazur, C.J. Rhodes, J. Telser, Role of oxygen radicals in DNA damage and cancer incidence, Mol. Cell. Biochem. 266 (2004) 37–56, https://doi.org/10.1023/b:mcbi.0000049134.69131.89.
[15] U.S. Srinivas, B.W.Q. Tan, B.A. Vellayappan, A.D. Jeyasekharan, ROS and the DNA damage response in cancer, Redox Biol. 25 (2019) 101084, https://doi.org/10.1016/j.redox.2018.101084.
[16] A. Valavanidis, T. Vlachogianni, C. Fiotakis, 8-hydroxy-2' -deoxyguanosine (8-OHdG): a critical biomarker of oxidative stress and carcinogenesis, J. Environ. Sci. Health C Environ. Carcinog. Ecotoxicol. Rev. 27 (2009) 120–139, https://doi.org/10.1080/10590500902885684.
[17] K. Kawai, H. Kasai, Y.-S. Li, Y. Kawasaki, S. Watanabe, M. Ohta, T. Honda, H. Yamato, Measurement of 8-hydroxyguanine as an oxidative stress biomarker in saliva by HPLC-ECD, Genes Environ 40 (2018), https://doi.org/10.1186/s41021-018-0095-2.
[18] S. Koide, Y. Kinoshita, N. Ito, J. Kimura, K. Yokoyama, I. Karube, Determination of human serum 8-hydroxy-2'-deoxyguanosine (8-OHdG) by HPLC-ECD combined with solid phase extraction (SPE), J. Chromatogr. B Analyt. Technol. Biomed. Life Sci. 878 (2010) 2163–2167, https://doi.org/10.1016/j.jchromb.2010.06.015.
[19] H. Kasai, A new automated method to analyze urinary 8-hydroxydeoxyguanosine by a high-performance liquid chromatography-electrochemical detector system, J. Radiat. Res. 44 (2003) 185–189, https://doi.org/10.1269/jrr.44.185.
[20] B.T. Nguyen, J.-C. Pyun, S.-G. Lee, M.-J. Kang, Identification of new binding proteins of focal adhesion kinase using immunoprecipitation and mass spectrometry, Sci. Rep. 9 (2019) 12908, https://doi.org/10.1038/s41598-019-49145-6.
[21] N.R. Jena, P.C. Mishra, Is FapyG mutagenic?: evidence from the DFT study, ChemPhysChem 14 (2013) 3263–3270, https://doi.org/10.1002/cphc.201300535.
[22] J.-P. Pouget, T. Douki, M.-J. Richard, J. Cadet, DNA damage induced in cells by γ and UVA radiation as measured by HPLC/GC−MS and HPLC−EC and comet assay, Chem. Res. Toxicol. 13 (2000) 541–549, https://doi.org/10.1021/tx000020e.
[23] P.L. Fischhaber, V.L. Gerlach, W.J. Feaver, Z. Hatahet, S.S. Wallace, E. C. Friedberg, Human DNA polymerase kappa bypasses and extends beyond thymine glycols during translesion synthesis in vitro, preferentially incorporating correct nucleotides, J. Biol. Chem. 277 (2002) 37604–37611, https://doi.org/10.1074/jbc.M206027200.
[24] N.G. Dolinnaya, E.A. Kubareva, E.A. Romanova, R.M. Trikin, T.S. Oretskaya, Thymidine glycol: the effect on DNA molecular structure and enzymatic processing, Biochimie 95 (2013) 134–147, https://doi.org/10.1016/j.biochi.2012.09.008.
[25] L. Hu, Z. Wang, C. Carmone, J. Keijer, D. Zhang, Role of oxidative DNA damage and repair in atrial fibrillation and ischemic heart disease, Int. J. Mol. Sci. 22 (2021) 3838, https://doi.org/10.3390/ijms22083838.
[26] D.B. Naritsin, S.P. Markey, Assessment of DNA oxidative damage by quantification of thymidine glycol residues using gas chromatography/electron capture negative ionization mass spectrometry, Anal. Biochem. 241 (1996) 35–41, https://doi.org/10.1006/abio.1996.0374.
[27] X.C. Le, J.Z. Xing, J. Lee, S.A. Leadon, M. Weinfeld, Inducible repair of thymine glycol detected by an ultrasensitive assay for DNA damage, Science 280 (1998) 1066–1069, https://doi.org/10.1126/science.280.5366.1066.
[28] S. DeVito, J. Woodrick, L. Song, R. Roy, Mutagenic potential of hypoxanthine in live human cells, Mutat, Res. 803–805 (2017) 9–16, https://doi.org/10.1016/j.mrfmmm.2017.06.005.
[29] A. Horváth, B.G. Vértessy, A one-step method for quantitative determination of uracil in DNA by real-time PCR, Nucleic Acids Res. 38 (2010) e196, https://doi.org/10.1093/nar/gkq815.
[30] Z. Zhang, R.T.K. Kwok, Y. Yu, B.Z. Tang, K.M. Ng, Aggregation-induced emission luminogen-based fluorescence detection of hypoxanthine: a probe for biomedical diagnosis of energy metabolism-related conditions, J. Mater. Chem. B 6 (2018) 4575–4578, https://doi.org/10.1039/c8tb00803e.
[31] H. Cong, H. Ding, G. Wang, X. Wang, L. Chen, Smartphone-assisted multicolor hypoxanthine sensing for on-site freshness assessment of aquatic products, Sens. Actuators B Chem. 379 (2023) 133246, https://doi.org/10.1016/j.snb.2022.133246.
[32] S. Hu, C. Xu, J. Luo, J. Luo, D. Cui, Biosensor for detection of hypoxanthine based on xanthine oxidase immobilized on chemically modified carbon paste electrode, Anal. Chim. Acta 412 (2000) 55–61, https://doi.org/10.1016/s0003-2670(00)00748-0.
[33] X. Wang, Z.-Z. Lin, C.-Y. Hong, Z.-Y. Huang, Colorimetric detection of hypoxanthine in aquatic products based on the enzyme mimic of cobalt-doped carbon nitride, New J. Chem. 45 (2021) 18307–18314, https://doi.org/10.1039/d1nj03467g.
[34] K.M. Amidon, B.F. Eichman, Structural biology of DNA abasic site protection by SRAP proteins, DNA Repair 94 (2020) 102903, https://doi.org/10.1016/j.dnarep.2020.102903.
[35] M. Talpaert-Borl≐, M. Liuzzi, Reaction of apurinic/apyrimidinic sites with [14C] methoxyamine, Biochim. Biophys. Acta, Gene Struct. Expression 740 (1983) 410–416, https://doi.org/10.1016/0167-4781(83)90089-1.
[36] L.H. Sanders, J. McCoy, X. Hu, P.G. Mastroberardino, B.C. Dickinson, C.J. Chang, C.T. Chu, B. Van Houten, J.T. Greenamyre, Mitochondrial DNA damage: molecular marker of vulnerable nigral neurons in Parkinson's disease, Neurobiol. Dis. 70 (2014) 214–223, https://doi.org/10.1016/j.nbd.2014.06.014.
[37] Y.W. Kow, A. Dare, Detection of abasic sites and oxidative DNA base damage using an ELISA-like assay, Methods 22 (2000) 164–169, https://doi.org/10.1006/meth.2000.1057.
[38] W. Lai, H. Wang, Detection and quantification of UV-irradiation-induced DNA damages by liquid chromatography-mass spectrometry and immunoassay, Photochem. Photobiol. 98 (2022) 598–608, https://doi.org/10.1111/php.13546.
[39] S.-I. Kim, S.-G. Jin, G.P. Pfeifer, Formation of cyclobutane pyrimidine dimers at dipyrimidines containing 5-hydroxymethylcytosine, Photochem. Photobiol. Sci. 12 (2013) 1409–1415, https://doi.org/10.1039/c3pp50037c.
[40] G.P. Pfeifer, R. Drouin, A.D. Riggs, G.P. Holmquist, In vivo mapping of a DNA adduct at nucleotide resolution: detection of pyrimidine (6-4) pyrimidone photoproducts by ligation-mediated polymerase chain reaction, Proc. Natl. Acad. Sci. U. S. A. 88 (1991) 1374–1378, https://doi.org/10.1073/pnas.88.4.1374.
[41] M. Karbaschi, N.J. Brady, M.D. Evans, M.S. Cooke, Immuno-slot blot assay for detection of UVR-mediated DNA damage, Methods Mol. Biol. 920 (2012) 163–175, https://doi.org/10.1007/978-1-61779-998-3_12.
[42] B. Steurer, Y. Turkyilmaz, M. van Toorn, W. van Leeuwen, P. Escudero-Ferruz, J. A. Marteijn, Fluorescently-labelled CPD and 6-4PP photolyases: new tools for live-cell DNA damage quantification and laser-assisted repair, Nucleic Acids Res. 47 (2019) 3536–3549, https://doi.org/10.1093/nar/gkz035.
[43] V. Savic, B. Yin, N.L. Maas, A.L. Bredemeyer, A.C. Carpenter, B.A. Helmink, K. S. Yang-Iott, B.P. Sleckman, C.H. Bassing, Formation of dynamic gamma-H2AX domains along broken DNA strands is distinctly regulated by ATM and MDC1 and dependent upon H2AX densities in chromatin, Mol. Cell 34 (2009) 298–310, https://doi.org/10.1016/j.molcel.2009.04.012.
[44] H. Qian, R.A. Hoebe, M.R. Faas, M.J. van Goethem, E.R. van der Graaf, C. Meyer, H. Kiewiet, S. Brandenburg, P.M. Krawczyk, A simple microscopy setup for visualizing cellular responses to DNA damage at particle accelerator facilities, Sci. Rep. 11 (2021) 14528, https://doi.org/10.1038/s41598-021-92950-1.
[45] A. Nakamura, O.A. Sedelnikova, C. Redon, D.R. Pilch, N.I. Sinogeeva, R. Shroff, M. Lichten, W.M. Bonner, Techniques for γ-H2AX detection, in: DNA Repair, Part B, Elsevier, 2006, pp. 236–250.
[46] C.E. Redon, J.S. Dickey, W.M. Bonner, O.A. Sedelnikova, γ-H2AX as a biomarker of DNA damage induced by ionizing radiation in human peripheral blood lymphocytes and artificial skin, Adv. Space Res. 43 (2009) 1171–1178, https://doi.org/10.1016/j.asr.2008.10.011.
[47] K. Brzozowska, M. Pinkawa, M.J. Eble, W.-U. Müller, A. Wojcik, R. Kriehuber, S. Schmitz, In vivo versus in vitro individual radiosensitivity analysed in healthy donors and in prostate cancer patients with and without severe side effects after radiotherapy, Int. J. Radiat. Biol. 88 (2012) 405–413, https://doi.org/10.3109/09553002.2012.666002.
[48] M.S. Siddiqui, M. François, M.F. Fenech, W.R. Leifert, γH2AX responses in human buccal cells exposed to ionizing radiation: ΓH2AX Response to Ionizing Radiation in Buccal Cells, Cytometry A 87 (2015) 296–308, https://doi.org/10.1002/cyto.a.22607.
[49] M.S. Siddiqui, M. François, M.F. Fenech, W.R. Leifert, Persistent γH2AX: a promising molecular marker of DNA damage and aging, Mutat. Res. Rev. Mutat. Res. 766 (2015) 1–19, https://doi.org/10.1016/j.mrrev.2015.07.001.
[50] D.M. Drake, A.M. Shapiro, P.G. Wells, Measurement of the oxidative DNA lesion 8-oxoguanine (8-oxoG) by ELISA or by high-performance liquid chromatography (HPLC) with electrochemical detection, Methods Mol. Biol. 1965 (2019) 313–328, https://doi.org/10.1007/978-1-4939-9182-2_21.
[51] J. Serrano, C.M. Palmeira, K.B. Wallace, D.W. Kuehl, Determination of 8-hydroxydeoxyguanosine in biological tissue by liquid chromatography/electrospray ionization-mass spectrometry/mass spectrometry, Rapid Commun. Mass Spectrom. 10 (1996) 1789–1791, https://doi.org/10.1002/(SICI)1097-0231(199611)10:14<1789::AID-RCM752>3.0.CO, 2-6.
[52] M. Weinfeld, K.J.M. Soderlind, Phosphorus-32-postlabeling detection of radiation-induced DNA damage: identification and estimation of thymine glycols and phosphoglycolate termini, Biochemistry 30 (1991) 1091–1097, https://doi.org/10.1021/bi00218a031.
[53] D.T. Bailey, H.-C.C. DeFedericis, K.F. Greene, H. Iijima, E.E. Budzinski, H. B. Patrzyc, J.B. Dawidzik, H.C. Box, A novel approach to DNA damage assessments: measurement of the thymine glycol lesion, Radiat. Res. 165 (2006) 438–444, https://doi.org/10.1667/rr3534.1.
[54] R. Boulieu, C. Bory, P. Baltassat, C. Gonnet, High-performance liquid chromatographic determination of hypoxanthine and xanthine in biological fluids, J. Chromatogr. 233 (1982) 131–140, https://doi.org/10.1016/s0378-4347(00)81739-9.
[55] M. Talpaert-Borlé, Formation, detection and repair of AP sites, Mutat. Res. 181 (1987) 45–56, https://doi.org/10.1016/0027-5107(87)90286-7.
[56] J. Nakamura, V.E. Walker, P.B. Upton, S.Y. Chiang, Y.W. Kow, J.A. Swenberg, Highly sensitive apurinic/apyrimidinic site assay can detect spontaneous and chemically induced depurination under physiological conditions, Cancer Res. 58 (1998) 222–225.
[57] K. Kubo, H. Ide, S.S. Wallace, Y.W. Kow, A novel, sensitive, and specific assay for abasic sites, the most commonly produced DNA lesion, Biochemistry 31 (1992) 3703–3708, https://doi.org/10.1021/bi00129a020.
[58] A. Besaratinia, G.P. Pfeifer, Measuring the formation and repair of UV damage at the DNA sequence level by ligation-mediated PCR, Methods Mol. Biol. 920 (2012) 189–202, https://doi.org/10.1007/978-1-61779-998-3_14.
[59] R. Nagarajan, G. Muthusamy, A. Balupillai, K. Govindasamy, K. Ramasamy, V. Ponniresan, I. Malla, Modified comet assays for the detection of cyclobutane pyrimidine dimers and oxidative base damages, J. Radiat. Canc. Res. 8 (2017) 82, https://doi.org/10.4103/0973-0168.199312.

[60] G.P. Pfeifer, R. Drouin, A.D. Riggs, G.P. Holmquist, Binding of transcription factors creates hot spots for UV photoproducts in vivo, Mol. Cell Biol. 12 (1992) 1798–1804, https://doi.org/10.1128/mcb.12.4.1798-1804.1992.
[61] N. Goto, G. Bazar, Z. Kovacs, M. Kunisada, H. Morita, S. Kizaki, H. Sugiyama, R. Tsenkova, C. Nishigori, Detection of UV-induced cyclobutane pyrimidine dimers by near-infrared spectroscopy and aquaphotomics, Sci. Rep. 5 (2015) 11808, https://doi.org/10.1038/srep11808.
[62] S. Li, R. Waters, Accelerated paper: nucleotide level detection of cyclobutane pyrimidine dimers using oligonucleotides and magnetic beads to facilitate labelling of DNA fragments incised at the dimers and chemical sequencing reference ladders, Carcinogenesis 17 (1996) 1549–1552, https://doi.org/10.1093/carcin/17.8.1549.
[63] U. Kasten, D. Beyersmann, J. Dahm-Daphi, A. Hartwig, Sensitive nonradioactive detection of UV-induced cyclobutane pyrimidine dimers in intact mammalian cells, Mutat. Res. 336 (1995) 143–152, https://doi.org/10.1016/0921-8777(94)00052-8.
[64] W. Yang, Structure and mechanism for DNA lesion recognition, Cell Res. 18 (2008) 184–197, https://doi.org/10.1038/cr.2007.116.
[65] S.S. David, V.L. O'Shea, S. Kundu, Base-excision repair of oxidative DNA damage, Nature 447 (2007) 941–950, https://doi.org/10.1038/nature05978.
[66] T. Visnes, A. Cázares-Körner, W. Hao, O. Wallner, G. Masuyer, O. Loseva, O. Mortusewicz, E. Wiita, A. Sarno, A. Manoilov, J. Astorga-Wells, A.-S. Jemth, L. Pan, K. Sanjiv, S. Karsten, C. Gokturk, M. Grube, E.J. Homan, B.M.F. Hanna, C. B.J. Paulin, T. Pham, A. Rasti, U.W. Berglund, C. von Nicolai, C. Benitez-Buelga, T. Koolmeister, D. Ivanic, P. Iliev, M. Scobie, H.E. Krokan, P. Baranczewski, P. Artursson, M. Altun, A.J. Jensen, C. Kalderén, X. Ba, R.A. Zubarev, P. Stenmark, I. Boldogh, T. Helleday, Small-molecule inhibitor of OGG1 suppresses proinflammatory gene expression and inflammation, Science 362 (2018) 834–839, https://doi.org/10.1126/science.aar8048.
[67] Q. Zhang, S. Zhao, X. Tian, J.-G. Qiu, C.-Y. Zhang, Development of a CRISPR-Cas-based biosensor for rapid and sensitive detection of 8-oxoguanine DNA glycosylase, Anal. Chem. 94 (2022) 2119–2125, https://doi.org/10.1021/acs.analchem.1c04453.
[68] S.-C. Liu, H.-W. Wu, J.-H. Jiang, G.-L. Shen, R.-Q. Yu, A novel DNAzyme-based colorimetric assay for the detection of hOGG1 activity with lambda exonuclease cleavage, Anal. Methods 5 (2013) 164–168, https://doi.org/10.1039/c2ay26018b.
[69] J. Shang, Z. Li, L. Liu, D. Xi, H. Wang, Label-free sensing of human 8-oxoguanine DNA glycosylase activity with a nanopore, ACS Sens. 3 (2018) 512–518, https://doi.org/10.1021/acssensors.7b00954.
[70] N.A. Kuznetsov, Y.N. Vorobjev, L.N. Krasnoperov, O.S. Fedorova, Thermodynamics of the multi-stage DNA lesion recognition and repair by formamidopyrimidine-DNA glycosylase using pyrrolocytosine fluorescence–stopped-flow pre-steady-state kinetics, Nucleic Acids Res. 40 (2012) 7384–7392, https://doi.org/10.1093/nar/gks423.
[71] J. Song, F. Yin, X. Li, N. Dong, Y. Zhu, Y. Shao, B. Chen, W. Jiang, C.-Z. Li, Sensitive detection of formamidopyrimidine-DNA glycosylase activity based on target-induced self-primed rolling circle amplification and magnetic nanoprobes, Analyst 143 (2018) 1593–1598, https://doi.org/10.1039/c7an02032e.
[72] J. Li, M. Zhang, H. Wang, J. Wu, R. Zheng, J. Zhang, Y. Li, Z. Wang, Z. Dai, Sensitive determination of formamidopyrimidine DNA glucosylase based on phosphate group-modulated multi-enzyme catalysis and fluorescent copper nanoclusters, Analyst 145 (2020) 5174–5179, https://doi.org/10.1039/d0an00928h.
[73] Y. Qiu, W. Dang, J. Fan, T. Zhou, B. Li, Y. Liu, Y. Qin, C. Tong, M. Daniyal, W. Wang, B. Liu, DNAzyme and rGO based fluorescence assay for Fpg activity analysis, drug screening, and bacterial imaging, Talanta 218 (2020) 121158, https://doi.org/10.1016/j.talanta.2020.121158.
[74] L. Das, V.G. Quintana, J.B. Sweasy, NTHL1 in genomic integrity, aging and cancer, DNA Repair 93 (2020) 102920, https://doi.org/10.1016/j.dnarep.2020.102920.
[75] I.V. Alekseeva, A.A. Kuznetsova, O.A. Kladova, V.O. Shender, P.V. Schneider, O. S. Fedorova, N.A. Kuznetsov, DNA probes for analysis of the activity of key enzymes of the base excision DNA repair pathway in human cells, Mol. Biol. 57 (2023) 299–311, https://doi.org/10.1134/s0026893323020024.
[76] T. Lindahl, Instability and decay of the primary structure of DNA, Nature 362 (1993) 709–715, https://doi.org/10.1038/362709a0.
[77] Y.-J. Lu, D.-P. Hu, Q. Deng, Z.-Y. Wang, B.-H. Huang, Y.-X. Fang, K. Zhang, W.-L. Wong, Sensitive and selective detection of uracil-DNA glycosylase activity with a new pyridinium luminescent switch-on molecular probe, Analyst 140 (2015) 5998–6004, https://doi.org/10.1039/c5an01158b.
[78] T. Squillaro, M. Finicelli, N. Alessio, S. Del Gaudio, G. Di Bernardo, M.A. B. Melone, G. Peluso, U. Galderisi, A rapid, safe, and quantitative in vitro assay for measurement of uracil-DNA glycosylase activity, J. Mol. Med. 97 (2019) 991–1001, https://doi.org/10.1007/s00109-019-01788-8.
[79] P.J. O'Brien, T. Ellenberger, Human alkyladenine DNA glycosylase uses acid-base catalysis for selective excision of damaged purines, Biochemistry 42 (2003) 12418–12429, https://doi.org/10.1021/bi035177v.
[80] S. Jang, N. Kumar, M.A. Schaich, Z. Zhong, B. van Loon, S.C. Watkins, B. Van Houten, Cooperative interaction between AAG and UV-DDB in the removal of modified bases, Nucleic Acids Res. 50 (2022) 12856–12871, https://doi.org/10.1093/nar/gkac1145.
[81] L. Wang, H. Zhang, Y. Xie, H. Chen, C. Ren, X. Chen, Target-mediated hyperbranched amplification for sensitive detection of human alkyladenine DNA glycosylase from HeLa cells, Talanta 194 (2019) 846–851, https://doi.org/10.1016/j.talanta.2018.10.083.
[82] M. Liu, N. Zhong, L. Zhang, Q. Zhang, X. Tian, F. Ma, C.-Y. Zhang, Single probe-based catalytic quantum dot FRET nanosensor for human alkyladenine DNA glycosylase detection, Talanta 266 (2024) 125089, https://doi.org/10.1016/j.talanta.2023.125089.
[83] H. Zhang, L. Wang, Y. Xie, X. Zuo, H. Chen, X. Chen, Base excision repair mediated cascading triple-signal amplification for the sensitive detection of human alkyladenine DNA glycosylase, Analyst 144 (2019) 3064–3071, https://doi.org/10.1039/c9an00200f.
[84] B. Demple, J.-S. Sung, Molecular and biological roles of Ape1 protein in mammalian base excision repair, DNA Repair 4 (2005) 1442–1449, https://doi.org/10.1016/j.dnarep.2005.09.004.
[85] Y. Hu, Z. Zhang, W. Ye, W. Zhang, M. Hu, W. Yuan, H. Wang, X. Xiao, T. Wu, A DNA structure-mediated fluorescent biosensor for apurinic/apyrimidinic endonuclease 1 activity detection with ultra-high sensitivity and selectivity, Sens. Actuators B Chem. 330 (2021) 129332, https://doi.org/10.1016/j.snb.2020.129332.
[86] X. Li, M. Xiong, Y. Huang, L. Zhang, S. Zhao, Simple label-free fluorescence detection of apurinic/apyrimidinic endonuclease 1 activity and its inhibitor using the abasic site-binding fluorophore, Anal. Methods 11 (2019) 739–743, https://doi.org/10.1039/c8ay02633e.
[87] N.M. Kad, H. Wang, G.G. Kennedy, D.M. Warshaw, B. Van Houten, Collaborative dynamic DNA scanning by nucleotide excision repair proteins investigated by single- molecule imaging of quantum-dot-labeled proteins, Mol. Cell 37 (2010) 702–713, https://doi.org/10.1016/j.molcel.2010.02.003.
[88] M. Kusakabe, Y. Onishi, H. Tada, F. Kurihara, K. Kusao, M. Furukawa, S. Iwai, M. Yokoi, W. Sakai, K. Sugasawa, Mechanism and regulation of DNA damage recognition in nucleotide excision repair, Genes Environ 41 (2019) 2, https://doi.org/10.1186/s41021-019-0119-6.
[89] S. Matsumoto, E.S. Fischer, T. Yasuda, N. Dohmae, S. Iwai, T. Mori, R. Nishi, K.-I. Yoshino, W. Sakai, F. Hanaoka, N.H. Thomä, K. Sugasawa, Functional regulation of the DNA damage-recognition factor DDB2 by ubiquitination and interaction with xeroderma pigmentosum group C protein, Nucleic Acids Res. 43 (2015) 1700–1713, https://doi.org/10.1093/nar/gkv038.
[90] S. Jang, N. Kumar, E.C. Beckwitt, M. Kong, E. Fouquerel, V. Rapić-Otrin, R. Prasad, S.C. Watkins, C. Khuu, C. Majumdar, S.S. David, S.H. Wilson, M. P. Bruchez, P.L. Opresko, B. Van Houten, Damage sensor role of UV-DDB during base excision repair, Nat. Struct. Mol. Biol. 26 (2019) 695–703, https://doi.org/10.1038/s41594-019-0261-7.
[91] J. Fei, N. Kaczmarek, A. Luch, A. Glas, T. Carell, H. Naegeli, Regulation of nucleotide excision repair by UV-DDB: prioritization of damage recognition to internucleosomal DNA, PLoS Biol. 9 (2011) e1001183, https://doi.org/10.1371/journal.pbio.1001183.
[92] V. Tiwari, B.A. Baptiste, M.N. Okur, V.A. Bohr, Current and emerging roles of Cockayne syndrome group B (CSB) protein, Nucleic Acids Res. 49 (2021) 2418–2434, https://doi.org/10.1093/nar/gkab085.
[93] J. Kapr, I. Scharkin, H. Ramachandran, P. Westhoff, M. Pollet, S. Dangeleit, G. Brockerhoff, A. Rossi, K. Koch, J. Krutmann, E. Fritsche, HiPSC-derived 3D neural models reveal neurodevelopmental pathomechanisms of the Cockayne Syndrome B, Cell. Mol. Life Sci. 81 (2024) 368, https://doi.org/10.1007/s00018-024-05406-w.
[94] C. Kroon, L. Breuer, L. Jones, J. An, A. Akan, E.A. Mohamed Ali, F. Busch, M. Fislage, B. Ghosh, M. Hellrigel-Holderbaum, V. Kazezian, A. Koppold, C. A. Moreira Restrepo, N. Riedel, L. Scherschinski, F.R. Urrutia Gonzalez, T. L. Weissgerber, Blind spots on western blots: assessment of common problems in western blot figures and methods reporting with recommendations to improve them, PLoS Biol. 20 (2022) e3001783, https://doi.org/10.1371/journal.pbio.3001783.
[95] L.A. Lindsey-Boltz, Y. Yang, C. Kose, N. Deger, K. Eynullazada, H. Kawara, A. Sancar, Nucleotide excision repair in Human cell lines lacking both XPC and CSB proteins, Nucleic Acids Res. 51 (2023) 6238–6245, https://doi.org/10.1093/nar/gkad334.
[96] R. Scully, A. Panday, R. Elango, N.A. Willis, DNA double-strand break repair-pathway choice in somatic mammalian cells, Nat. Rev. Mol. Cell Biol. 20 (2019) 698–714, https://doi.org/10.1038/s41580-019-0152-0.
[97] Z. Qi, S. Redding, J.Y. Lee, B. Gibb, Y. Kwon, H. Niu, W.A. Gaines, P. Sung, E. C. Greene, DNA sequence alignment by microhomology sampling during homologous recombination, Cell 160 (2015) 856–869, https://doi.org/10.1016/j.cell.2015.01.029.
[98] J.R. Walker, R.A. Corpina, J. Goldberg, Structure of the Ku heterodimer bound to DNA and its implications for double-strand break repair, Nature 412 (2001) 607–614, https://doi.org/10.1038/35088000.
[99] M. Liu, S. Rehman, X. Tang, K. Gu, Q. Fan, D. Chen, W. Ma, Methodologies for improving HDR efficiency, Front. Genet. 9 (2018) 691, https://doi.org/10.3389/fgene.2018.00691.
[100] K.-J. Lee, J. Saha, J. Sun, K.R. Fattah, S.-C. Wang, B. Jakob, L. Chi, S.-Y. Wang, G. Taucher-Scholz, A.J. Davis, D.J. Chen, Phosphorylation of Ku dictates DNA double-strand break (DSB) repair pathway choice in S phase, Nucleic Acids Res. 44 (2016) 1732–1745, https://doi.org/10.1093/nar/gkv1499.
[101] S. Mukherjee, P. Chakraborty, P. Saha, Phosphorylation of Ku70 subunit by cell cycle kinases modulates the replication related function of Ku heterodimer, Nucleic Acids Res. 44 (2016) 7755–7765, https://doi.org/10.1093/nar/gkw622.
[102] S. Brandt, E.P. Samartzis, A.-K. Zimmermann, D. Fink, H. Moch, A. Noske, K. J. Dedes, Lack of MRE11-RAD50-NBS1 (MRN) complex detection occurs frequently in low-grade epithelial ovarian cancer, BMC Cancer 17 (2017) 44, https://doi.org/10.1186/s12885-016-3026-2.

[103] S. Magaki, S.A. Hojat, B. Wei, A. So, W.H. Yong, An introduction to the performance of immunohistochemistry, Methods Mol. Biol. 1897 (2019) 289–298, https://doi.org/10.1007/978-1-4939-8935-5_25.
[104] S. Matsuda, T. Ikura, T. Matsuda, Absolute quantification of DNA damage response proteins, Genes Environ 45 (2023) 37, https://doi.org/10.1186/s41021-023-00295-0.
[105] R. Aebersold, M. Mann, Mass spectrometry-based proteomics, Nature 422 (2003) 198–207, https://doi.org/10.1038/nature01511.
[106] J. Tchou, V. Bodepudi, S. Shibutani, I. Antoshechkin, J. Miller, A.P. Grollman, F. Johnson, Substrate specificity of Fpg protein. Recognition and cleavage of oxidatively damaged DNA, J. Biol. Chem. 269 (1994) 15318–15324, https://doi.org/10.1016/s0021-9258(17)36608-5.
[107] M. Hedglin, P.J. O'Brien, Human alkyladenine DNA glycosylase employs a processive search for DNA damage, Biochemistry 47 (2008) 11434–11445, https://doi.org/10.1021/bi801046y.
[108] A.L. Jacobs, P. Schär, DNA glycosylases: in DNA repair and beyond, Chromosoma 121 (2012) 1–20, https://doi.org/10.1007/s00412-011-0347-4.
[109] J.C. Park, S. Park, S. Bang, H. Kim, Y. Lee, M.G. Park, S.G. Yoon, Y. Jeong, H. Kim, S.H. Kang, K.H. Lee, Catapult-like DNA actuator for highly stable and ultrasensitive detection of urinary miRNA, Chem. Eng. J. 506 (2025) 159806, https://doi.org/10.1016/j.cej.2025.159806.
[110] C. Keum, H. Yeom, T.I. Noh, S.Y. Yi, S. Jin, C. Kim, J.S. Shim, S.G. Yoon, H. Kim, K.H. Lee, S.H. Kang, Y. Jeong, Diagnosis of early-stage bladder cancer via unprocessed urine samples at the point of care, Nat. Biomed. Eng. (2024), https://doi.org/10.1038/s41551-024-01298-0.
[111] G. Figueroa-González, C. Pérez-Plasencia, Strategies for the evaluation of DNA damage and repair mechanisms in cancer, Oncol. Lett. 13 (2017) 3982–3988, https://doi.org/10.3892/ol.2017.6002.
[112] M. Podhorecka, A. Skladanowski, P. Bozko, H2AX phosphorylation: its role in DNA damage response and cancer therapy, J. Nucleic Acids 2010 (2010), https://doi.org/10.4061/2010/920161.
[113] F.L. Monteiro, T. Baptista, F. Amado, R. Vitorino, C. Jerónimo, L.A. Helguero, Expression and functionality of histone H2A variants in cancer, Oncotarget 5 (2014) 3428–3443, https://doi.org/10.18632/oncotarget.2007.
[114] A.R. Baptistella, M.C. Landemberger, M.V.S. Dias, F.S. Giudice, B.R. Rodrigues, P. P.C.E. da Silva, E.K. Cassinela, T.C. Lacerda, F.A. Marchi, A.F.P. Leme, M. D. Begnami, S. Aguiar Jr., V.R. Martins, Rab5C enhances resistance to ionizing radiation in rectal cancer, J. Mol. Med. 97 (2019) 855–869, https://doi.org/10.1007/s00109-019-01760-6.
[115] S. Richman, Deficient mismatch repair: Read all about it (Review), Int. J. Oncol. 47 (2015) 1189–1202, https://doi.org/10.3892/ijo.2015.3119.
[116] Y. Park, S.K. Nam, S.H. Seo, K.U. Park, H.J. Oh, Y.S. Park, Y.-S. Suh, S.-H. Ahn, D. J. Park, H.-H. Kim, H.S. Lee, Comprehensive study of microsatellite instability testing and its comparison with immunohistochemistry in gastric cancers, J. Gastric Cancer 23 (2023) 264–274, https://doi.org/10.5230/jgc.2023.23.e5.
[117] A. Reddig, C.E. Rübe, S. Rödiger, P. Schierack, D. Reinhold, D. Roggenbuck, DNA damage assessment and potential applications in laboratory diagnostics and precision medicine, J. Lab. Precis. Med. 3 (2018), https://doi.org/10.21037/jlpm.2018.03.06, 31–31.
[118] J. Brownlie, S. Kulkarni, M. Algethami, J.N. Jeyapalan, N.P. Mongan, E.A. Rakha, S. Madhusudan, Targeting DNA damage repair precision medicine strategies in cancer, Curr. Opin. Pharmacol. 70 (2023) 102381, https://doi.org/10.1016/j.coph.2023.102381.
[119] S.H. Schurman, C.A. Dunn, R. Greaves, B. Yu, L. Ferrucci, D.L. Croteau, M. M. Seidman, V.A. Bohr, Age-related disease association of endogenous γ-H2AX foci in mononuclear cells derived from leukapheresis, PLoS One 7 (2012) e45728, https://doi.org/10.1371/journal.pone.0045728.
[120] L.J. Kuo, L.-X. Yang, Gamma-H2AX - a novel biomarker for DNA double-strand breaks, In Vivo (Athens) 22 (2008) 305–309.
[121] S. Ressler, J. Bartkova, H. Niederegger, J. Bartek, K. Scharffetter-Kochanek, P. Jansen-Dürr, M. Wlaschek, p16INK4A is a robust in vivo biomarker of cellular aging in human skin, Aging Cell 5 (2006) 379–389, https://doi.org/10.1111/j.1474-9726.2006.00231.x.
[122] Y. Liu, H.K. Sanoff, H. Cho, C.E. Burd, C. Torrice, J.G. Ibrahim, N.E. Thomas, N. E. Sharpless, Expression of p16(INK4a) in peripheral blood T-cells is a biomarker of human aging, Aging Cell 8 (2009) 439–448, https://doi.org/10.1111/j.1474-9726.2009.00489.x.
[123] M. Yousefzadeh, C. Henpita, R. Vyas, C. Soto-Palma, P. Robbins, L. Niedernhofer, DNA damage-how and why we age? Elife 10 (2021) https://doi.org/10.7554/eLife.62852.
[124] Y. Zhao, M. Simon, A. Seluanov, V. Gorbunova, DNA damage and repair in age-related inflammation, Nat. Rev. Immunol. 23 (2023) 75–89, https://doi.org/10.1038/s41577-022-00751-y.
[125] J. Guo, X. Huang, L. Dou, M. Yan, T. Shen, W. Tang, J. Li, Aging and aging-related diseases: from molecular mechanisms to interventions and treatments, Signal Transduct. Targeted Ther. 7 (2022) 391, https://doi.org/10.1038/s41392-022-01251-0.
[126] S.L. Spurgeon, R.C. Jones, R. Ramakrishnan, High throughput gene expression measurement with real time PCR in a microfluidic dynamic array, PLoS One 3 (2008) e1662, https://doi.org/10.1371/journal.pone.0001662.
[127] A.G. Condie, Y. Yan, S.L. Gerson, Y. Wang, A fluorescent probe to measure DNA damage and repair, PLoS One 10 (2015) e0131330, https://doi.org/10.1371/journal.pone.0131330.
[128] S. Zhu, J.A. Coffman, Simple and fast quantification of DNA damage by real-time PCR, and its application to nuclear and mitochondrial DNA from multiple tissues of aging zebrafish, BMC Res. Notes 10 (2017), https://doi.org/10.1186/s13104-017-2593-x.
[129] S. Adar, J. Hu, J.D. Lieb, A. Sancar, Genome-wide kinetics of DNA excision repair in relation to chromatin state and mutagenesis, Proc. Natl. Acad. Sci. U. S. A. 113 (2016) E2124–E2133, https://doi.org/10.1073/pnas.1603388113.
[130] F. Iannelli, A. Galbiati, I. Capozzo, Q. Nguyen, B. Magnuson, F. Michelini, G. D'Alessandro, M. Cabrini, M. Roncador, S. Francia, N. Crosetto, M. Ljungman, P. Carninci, F. d'Adda di Fagagna, A damaged genome's transcriptional landscape through multilayered expression profiling around in situ-mapped DNA double-strand breaks, Nat. Commun. 8 (2017) 15656, https://doi.org/10.1038/ncomms15656.
[131] B. Martinez-Pastor, G.G. Silveira, T.L. Clarke, D. Chung, Y. Gu, C. Cosentino, L. S. Davidow, G. Mata, S. Hassanieh, J. Salsman, A. Ciccia, N. Bae, M.T. Bedford, D. Megias, L.L. Rubin, A. Efeyan, G. Dellaire, R. Mostoslavsky, Assessing kinetics and recruitment of DNA repair factors using high content screens, Cell Rep. 37 (2021) 110176, https://doi.org/10.1016/j.celrep.2021.110176.
[132] J.Y. Choi, S. Park, J.S. Shim, H.J. Park, S.U. Kuh, Y. Jeong, M.G. Park, T.I. Noh, S. G. Yoon, Y.M. Park, S.J. Lee, H. Kim, S.H. Kang, K.H. Lee, Explainable artificial intelligence-driven prostate cancer screening using exosomal multi-marker based dual-gate FET biosensor, Biosens. Bioelectron. 267 (2025) 116773, https://doi.org/10.1016/j.bios.2024.116773.
[133] H. Kim, S. Park, I.G. Jeong, S.H. Song, Y. Jeong, C.-S. Kim, K.H. Lee, Noninvasive precision screening of prostate cancer by urinary multimarker sensor and artificial intelligence analysis, ACS Nano 15 (2021) 4054–4065, https://doi.org/10.1021/acsnano.0c06946.
[134] S. Wei, S. Shalhout, Y.-H. Ahn, A.S. Bhagwat, A versatile new tool to quantify abasic sites in DNA and inhibit base excision repair, DNA Repair 27 (2015) 9–18, https://doi.org/10.1016/j.dnarep.2014.12.006.
[135] Q. You, X. Feng, Y. Cai, S.B. Baylin, H. Li, Human 8-oxoguanine glycosylase OGG1 binds nucleosome at the dsDNA ends and the super-helical locations, Commun, Biol. 7 (2024) 1202, https://doi.org/10.1038/s42003-024-06919-7.
[136] K. Karanam, A. Loewer, G. Lahav, Dynamics of the DNA damage response: insights from live-cell imaging, Brief, Funct. Genomics 12 (2013) 109–117, https://doi.org/10.1093/bfgp/els059.
[137] M.K. Shigenaga, T.M. Hagen, B.N. Ames, Oxidative damage and mitochondrial decay in aging, Proc. Natl. Acad. Sci. U. S. A. 91 (1994) 10771–10778, https://doi.org/10.1073/pnas.91.23.10771.
[138] T. Tsujino, T. Takai, K. Hinohara, F. Gui, T. Tsutsumi, X. Bai, C. Miao, C. Feng, B. Gui, Z. Sztupinszki, A. Simoneau, N. Xie, L. Fazli, X. Dong, H. Azuma, A. D. Choudhury, K.W. Mouw, Z. Szallasi, L. Zou, A.S. Kibel, L. Jia, CRISPR screens reveal genetic determinants of PARP inhibitor sensitivity and resistance in prostate cancer, Nat. Commun. 14 (2023) 252, https://doi.org/10.1038/s41467-023-35880-y.
[139] A. Ragupathi, M. Singh, A.M. Perez, D. Zhang, Targeting the BRCA1/2 deficient cancer with PARP inhibitors: clinical outcomes and mechanistic insights, Front. Cell Dev. Biol. 11 (2023) 1133472, https://doi.org/10.3389/fcell.2023.1133472.
[140] P.C. Searson, The Cancer Moonshot, the role of in vitro models, model accuracy, and the need for validation, Nat. Nanotechnol. 18 (2023) 1121–1123, https://doi.org/10.1038/s41565-023-01486-0.